COMPUTER APPLICATIONS IN DERMATOLOGY

WILLIAM V. STOECKER, M.D.

Clinical Assistant Professor and Adjunct Assistant Professor
Division of Dermatology
Department of Internal Medicine
University of Missouri-Columbia
Columbia, Missouri
and
Department of Computer Science
University of Missouri-Rolla
Rolla, Missouri

IGAKU-SHOIN New York • Tokyo

ELEVEN QUANTITATIVE DERMATOPATHOLOGY[1,2]

Wilhelm Stolz, Thomas Vogt, Michael Landthaler, and Wolfgang Abmayr

LIST OF ABBREVIATIONS

AIDS	acquired immunodeficiency syndrome
CCM	computerized DNA cytometry
CPM	cytophotometry
CV	canonic variable
FC	flow cytometry
FHP	feature histogram percentage
IA	image analysis
ICM	interactive computerized morphometry
IOD	integrated optical density
KA	keratoacanthoma
KS	Kaposi's sarcoma
LP	lymphomatoid papulosis
MACs	markedly atypical cells
MF	mycosis fungoides
ML	malignant lymphoma
MM	malignant melanoma
MN	melanocytic nevi
PL	pseudolymphoma
SCC	squamous cell carcinoma
SD	standard deviation
2*c*DI	2*c* deviation index
4*c* ER, 5*c* ER	4*c* and 5*c* exceeding rate

> Dermatology will be morphology or it will cease to exist.
>
> —Oscar Gans

In dermatopathology it is important to recognize specific patterns that allow nosologic classification and discrimination between both benign and malignant lesions as well as different grades of malignancy. In tumors this naturally implies the quantitative assessment of cellular features (size, shape, chromatin structure) and architectural features (tumor thickness, invasiveness, inflammatory reaction of the host). It is therefore not surprising that the history of quantitative measurements in pathology had already started by 1851, when Lebert determined the diameters of cells and their nuclei and noted changes occurring in cancers.[1] Virchow also measured cancer cell dimensions and noted the pleomorphic nature of cancer cells and their nuclei.[2] In 1928, Cowdry[3] used the recently introduced Feulgen reaction[4] to investigate the chromatin content of normal and neoplastic cells, but his study was hampered by the lack of accurate instrumentation for quantitative measurements.

Quantification in traditional pathology occurs mainly at subconscious levels and therefore many intra- and interobserver differences in the evaluation of premalignant and malignant lesions have been reported.[5,6] The human eye–brain complex is highly optimized for the detection of edges or boundaries, which reflects the architectural constituents of the perceptive fields of the retinal ganglion cells and occipital cortical neurons. However, there are striking deficiencies in the human system in the recognition of absolute size or density information, very important in classifying histologic specimens. Moreover, we have problems in detecting small differences in either size or density of objects, particularly if they cannot be viewed close together so that a relative assessment can be made. Our visual system is also poor at recognizing higher-order statistical relationships in an image, such as those that occur within the texture of nuclear chromatin.[7] In many situations, of course, the diagnosis rendered by the dermatopathologist based on years of accumulated experience is highly reliable. Nevertheless, objective methods for the quantitative evaluation of cell and tissue features are required, especially if the differences are only slight.

[1] This chapter is dedicated to Otto Braun-Falco on his seventieth birthday.

[2] Supported by the Deutsche Forschungsgemeinschaft (Sto 189/1-1 and 1-2).

Therefore, several techniques have been introduced during recent decades to assist in dermatopathologic decisions. These include morphometry, the measurement of one- and two-dimensional geometric features from structural elements or particles;[8] stereology, a mathematical method for the assessment of the third dimension using data from one- or two-dimensional measurements;[9] cytophotometry;[10] and flow cytometry,[11] applying photometry and laser technique.

Because of the recent developments in computer technology, morphometric and densitometric measurements can now also be performed by digital image processing.[12] Digital imaging systems encode and process the entire visual information provided by a video camera. Currently, the term *image analysis* (IA) is used for many different techniques. In our opinion, the term *IA* should be restricted to procedures measuring gray values, for example, quantitative analyses of Feulgen-stained DNA or surface markers stained with monoclonal antibodies,[13–15] or digital IA used for the enhancement of original images prior to the calculation of one- and two-dimensional geometric features. If only morphometric measurements are performed, with the support of a computer, the term *interactive computerized morphometry* (ICM) should be preferred in order to avoid misinterpretations.[16]

In this chapter we will first clarify the terms of quantitative dermatopathology and subsequently discuss major fields of applications. We will emphasize studies improving the diagnosis and prognostic evaluation of malignant melanoma and malignant cutaneous non-Hodgkin's lymphoma on both the light microscopic and the ultrastructural levels. Further applications of image processing such as grain counting and three-dimensional reconstruction will also be discussed.

TECHNIQUES

Morphometry

Morphometry can be defined as the measurement of geometric features of any particles or cellular elements.[8] Thus this method can give an accurate, objective, and reproducible description of microscopic or macroscopic objects. The main features used for characterization of objects are shape, size, and spatial distribution.

Two morphometric techniques can be differentiated:

- Less expensive, nonautomatic routines using rulers, ocular micrometers, or grids for point or intercept counting.[8]
- Interactive computerized techniques using a digitizing tablet for interactive segmentation of objects by the use of a cursor or a pen (ICM).[16]

The selection of instrumentation strongly depends on the question to be analyzed. Point counting, the best-known technique in quantitative pathology, is appropriate for measurements of discrete events, for instance, the counting of mitotic figures within a microscopic field.[7] For accurate measurements of individual objects, ICM is required.

Stereology

Stereology is a special morphometric technique that applies mathematical formulas for the calculation of parameters in three dimensions.[9] A recent development in this field is the analysis of the volume-weighted mean nuclear volume, which is based on measurements of nuclear intercepts.[17] Briefly, in randomly selected sections the length of nuclear intercepts is proportional to the volume-weighted mean nuclear volume.

Image Analysis

Digital IA allows the most general approach to quantitative morphologic questions because of its unique capability to determine morphometric parameters, gray values, and color information simultaneously.[12] Thus computerized IA is very similar to human visual processing with the advantage of providing objective information and complex statistical evaluation.[18] In addition, the presence of microscopic images in a digital form enables storage and retrieval of images indefinitely. At present, the most frequent applications of IA in pathology concern studies for the improvement of diagnosis and prognostic evaluation of malignant tumors. The IA procedure consists of three major steps:

1. Identification of the boundaries of an object
2. Extraction of features

3. Classification of objects and specimens into defined categories

DNA measurements using IA. Since IA systems also provide densitometric information, the assessment of nuclear DNA content, an important feature for diagnostic and prognostic evaluation, is possible. The nuclear DNA content became of major interest in pathology in the 1950s with the discovery, by means of cytophotometry, of an increased DNA content in tumor tissues.[19,20] The prerequisite for cytophotometry is the application of a stoichiometric DNA-specific stain, which was first described by Feulgen and Rossenbeck in 1924.[4] Cytophotometry was first performed with difficult routines such as the *plug method* or the *two-wavelength technique,*[21] until scanning microscopes became available in the late 1960s. In the 1970s scanning cytophotometers were supplied with computers for control of scanning, data acquisition, and processing, already similar to video image analysis systems.[22] Because of the development of high-quality video cameras, cytophotometers were gradually replaced by video image analysis systems. Already, by 1968, Wied et al.[23] had introduced the novel *t*axonomic *i*ntra*c*ellular *a*nalytic *s*ystem (TICAS).

The first cytophotometric measurements in dermatopathology were performed by Kint on basal cell carcinoma and squamous cell carcinoma, disclosing aneuploid cells within the tumors.[24] This data was confirmed by Ehlers[25] and Manocha.[26] Aneuploid nuclei were also detected in reticulum cell sarcoma.[27] The first imprint specimens of melanocytic lesions were analyzed by Ehlers and coworkers, who detected highly aneuploid nuclei in malignant melanoma (MM).[28] Bloch and Goodman demonstrated aneuploidy in virus papillomas.[20,29] Simultaneous with the development of single-cell scanning cytophotometry, flow cytometry (FC) was developed beginning in the 1960s.[30,31] This method allows the measurement of large numbers of cells (>50,000) within a few minutes. A monodisperse suspension is prepared from fresh tissue or from paraffin blocks. The flow is arranged so that the cells singly pass the measuring stations. The measurements can be electronic, as in the Coulter counter, or optical, as in most flow cytometers. Using flow cytometers, one can measure the expression of cellular antigens, proteins, and enzyme activities, as well as some morphometric features. For detailed principles and applications of FC, see references 11, 32, and 33. Barlogie and coworkers first described aneuploidies in MM using FC.[34] The major drawback of the method is that small fractions of cells, for example, cells exceeding a DNA content of 5*c* (a normal diploid nucleus has a DNA content of 2*c*) cannot be recognized among a huge number of cells analyzed. In addition, the operator cannot visually control the object, and thus clumping of cells or stroma cells may disturb data analysis.[36]

DNA analysis by IA systems requires the segmentation of stained nuclei and the calculation of the integrated optical density (IOD). The IOD is the product of the optical density (calculated from the gray values of object pixels) and the area (number of object pixels). Figure 11-1 demonstrates the steps of automatic segmentation of nuclei for DNA measurements on imprints of malignant lymphomas. In Feulgen-stained nuclei, the IOD is linearly correlated with the DNA content.[20] By comparing the actual IOD value of reference cells, for example, chicken erythrocytes or normal human lymphocytes, a factor can be calculated that allows the determination of the relative DNA content from the IOD value measured in a cell. A normal diploid cell is characterized by a relative DNA value of 2.0, a euploid cell in G_2 phase contains DNA with a value of 4.0. Cells with values higher than 5.0 are definitely aneuploid, if polyploidization can be ruled out. Examples of nuclei from a malignant lymphoma, measured by *c*omputerized DNA *cy*to*m*etry (CCM)—this term should be used for DNA measurements by IA)—are shown in Figure 11-2.

The number of cells analyzed by CCM is much lower (50 to 200) than in FC, but IA allows the visual control of the objects measured. Thus single aneuploid nuclei can also be identified with high precision. Clumped or destroyed cells can be rejected, and then only cells of interest are measured. If tissue sections are analyzed, measurements can be restricted to nuclei in regions of special interest such as intraepidermal nuclei.[13]

The major applications of CCM will be discussed below.

Quantification of chromatin structure by IA. IA is also well suited for the quantification of the amount of eu- and heterochromatin and for the assessment of other chromatin features such as heterogeneity or

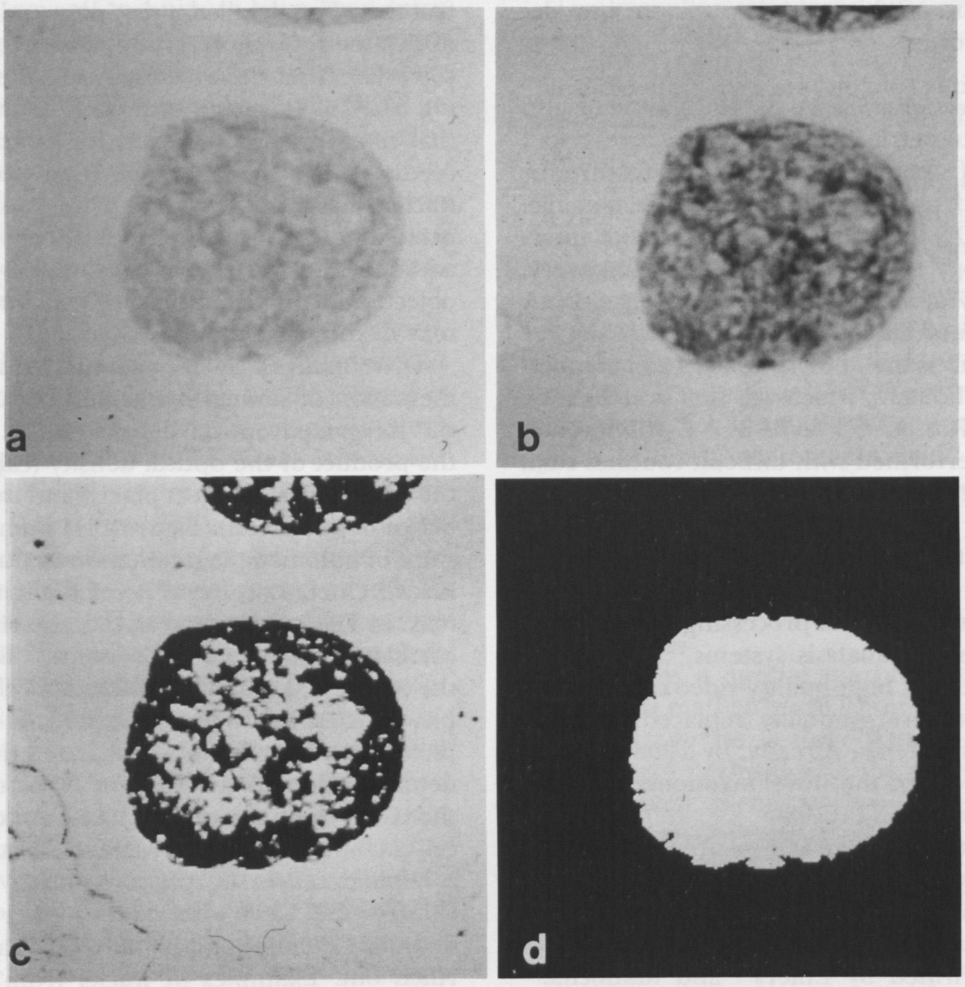

Fig. 11-1 Automatic segmentation. (a) Original image. (b) Image after mapping the actual gray values into the full range (normalization of the gray-value histogram). (c) Image after the application of an addition of the original with the difference between the original and the low-passed version of it. (d) Image after using a gray-value threshold of 130. Inaccurate segmentation could be rejected by giving the contour in the overlay of the original. Reprinted by permission of the Elsevier Science Publishing Co., Inc. from Stolz et al.[107] Copyright 1990 by the Society for Investigative Dermatology, Inc.

presence of dark aggregations. Suitable features for quantification of eu- and heterochromatin were described by Abmayr et al.[37] as the so-called feature histogram percentage (FHP) features, applicable also to electron microscopy. In Figures 11-3 and 11-4 the way the FHP-features were calculated is illustrated in a nucleus of a melanocytic nevus (Fig. 11-3) and a nucleus of a malignant melanoma (Fig. 11-4). In the beginning a gray-value histogram is determined in the difference image between the original and the median-filtered version of it. In these images gray values between 100 and 157 can be found. In order to facilitate statistical evaluation, three gray-value channels were summarized to one new gray value channel. The ratio of pixels within one gray-value channel to the total number of pixels within a nucleus is expressed as FHP. The original images are given in Figures 11-3a and 11-4a, the median-filtered versions in figures 11-3b and 11-4b, and the difference image

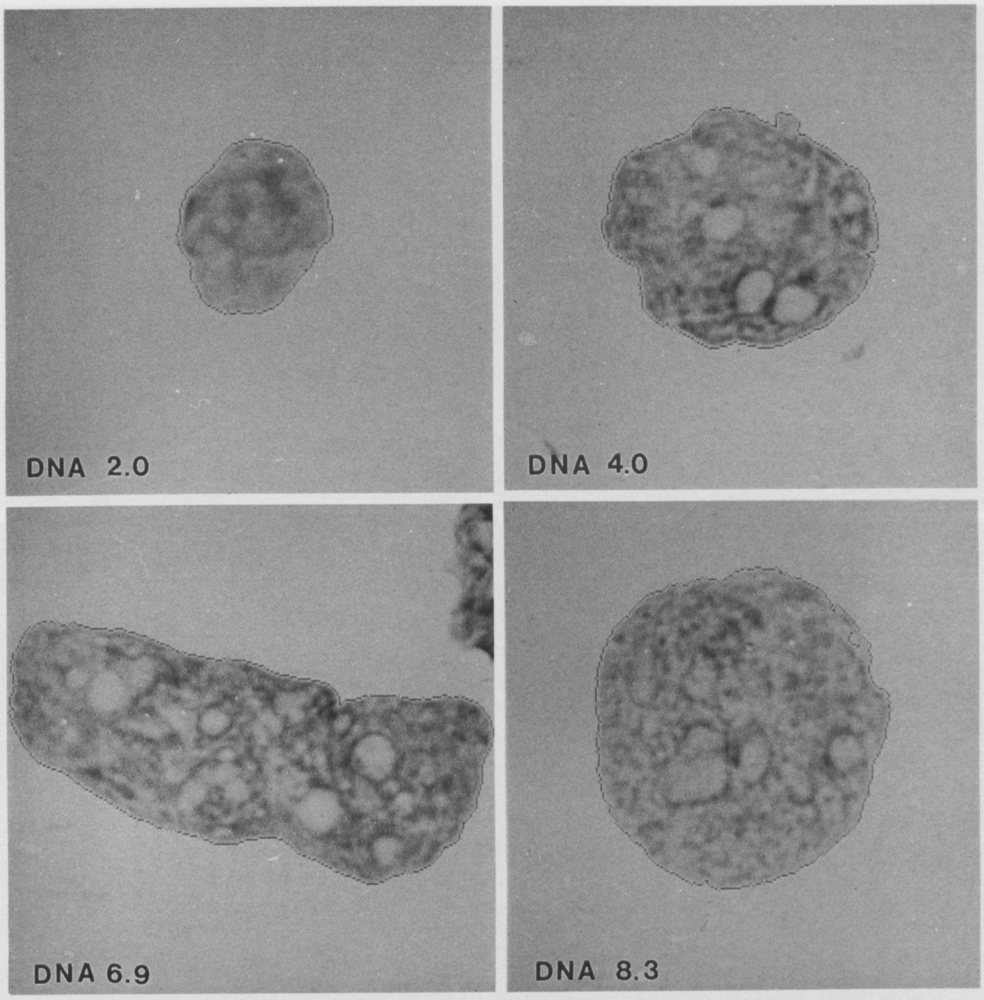

Fig. 11-2 Examples of nuclei with different relative DNA values measured by CCM. A normal diploid nucleus contains a relative DNA value of 2.0. Reprinted by permission of the Elsevier Science Publishing Co., Inc. from Stolz et al.[107] Copyright 1990 by the Society for Investigative Dermatology, Inc.

with an offset of 128 gray values in Figures 11-3c and 11-4c. In Figures 11-3d and 11-4d, heterochromatin is represented by the channels FHP 100 to FHP 121 and euchromatin by FHP 124 to FHP 154. The calculation of the difference image is necessary to get selective gray values for the chromatin particles and remove the nucleoli. Since nucleoli contain almost exclusively RNA, they should not be included for the calculation of pure DNA features such as hetero- and euchromatin.[38] For quantification of chromatin heterogeneity, features extracted from the cooccurrence matrix were applied. Only a brief outline can be given here; a more detailed description and the exact formulas are shown elsewhere.[39] The basic idea of the cooccurrence matrix is the transfer of the texture of any image to a mathematical square matrix. The elements of the matrix are proportional to the probability of finding pairs of data points in the image at given gray levels and specified spatial arrangements. Generally, in an inhomogenous image the probability of finding pairs outside the

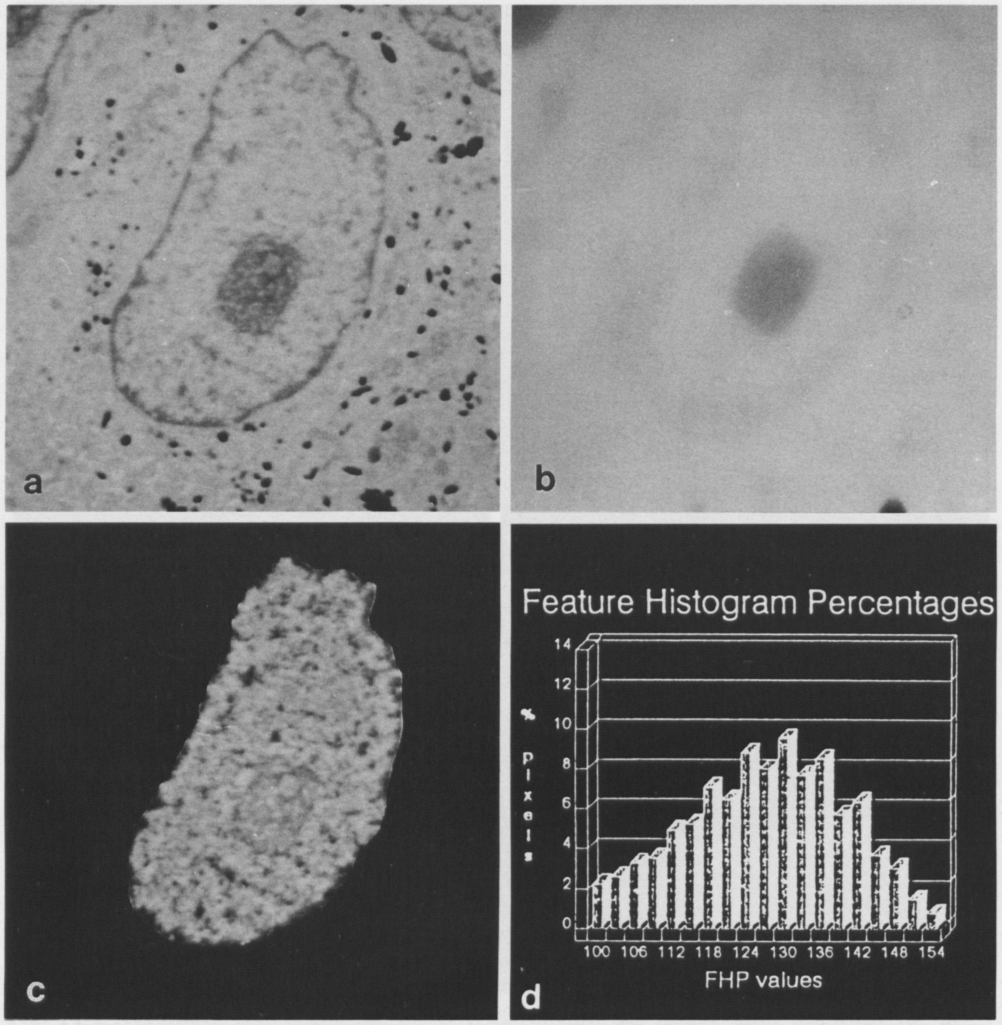

Fig. 11-3 Steps for calculation of FHP values demonstrated on a nucleus of a melanocytic nevus. (a) Normalized gray-level image. (b) Median-filtered (filter size 21 × 21 pixels) version of (a). (c) Difference between (a) and (b) with addition of a constant gray value of 128 for all pixels. (d) Gray-value histogram of the nucleus in (c); on the abscissa the different channels between black (100) and white (154) and on the ordinate the values of the FHPs for the various gray channels are given. Reprinted by permission of the Elsevier Science Publishing Co., Inc. from Stolz W et al. *J Invest Dermatol* 97:1–8, 1991. Copyright 1991 by the Society for Investigative Dermatology, Inc.

diagonal is greater than in a homogeneous one. Several cooccurrence features as contrast, correlation, variance, and entropy can be calculated.

Evaluation of in situ hybridization by image analysis. In situ hybridization is a unique technique for the detection of mRNA within cells.[40,41] Quantification of grain densities can be performed either by rough estimation or by exact counting of the grains. Within the first procedure, only striking differences can be detected; the latter is very time-consuming, IA can also improve the assessment of in situ hybridization results.[42]

Figure 11-5 demonstrates some essential steps of image processing for automatic grain counting. Initially, the contour of the cell is determined in

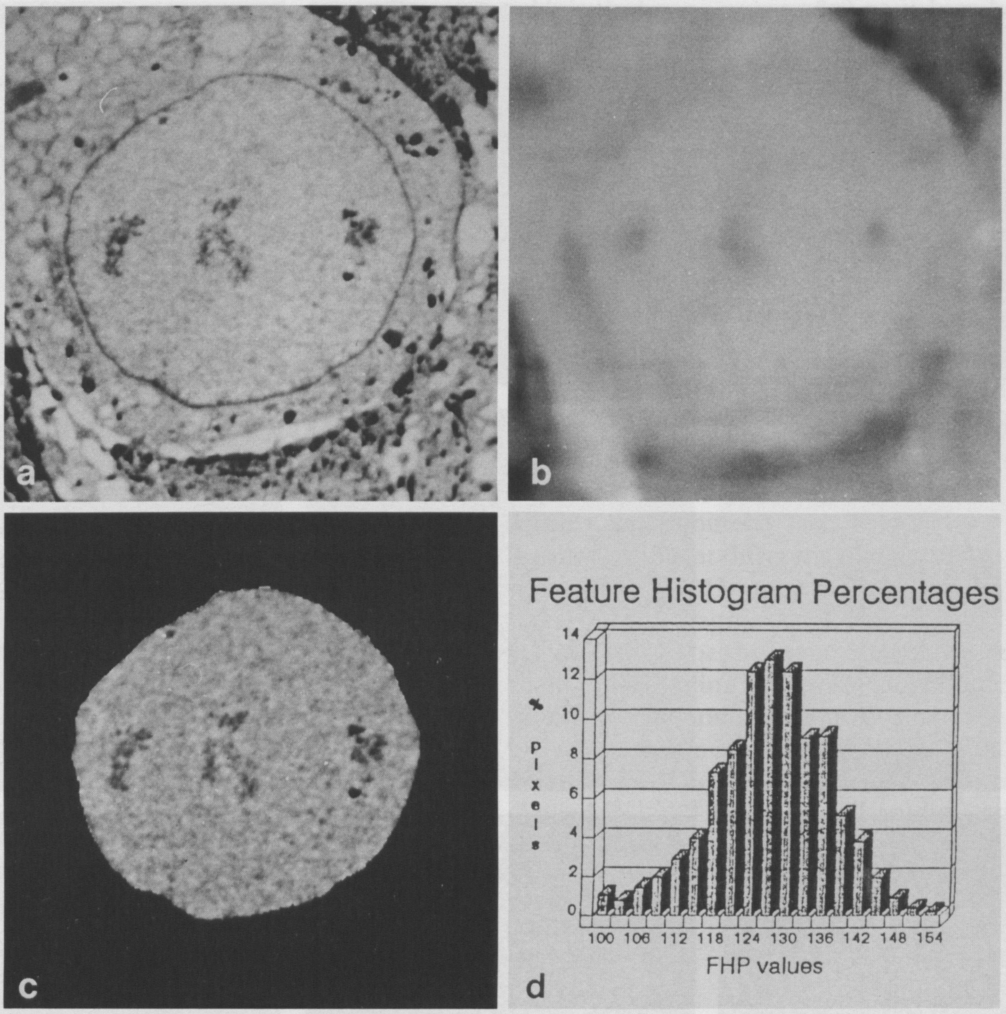

Fig. 11-4 Steps for calculation of FHP values demonstrated on a nucleus of an MM. For detailed explanation, see Fig. 11-3. Reprinted by permission of the Elsevier Science Publishing Co., Inc. from Stolz et al. *J Invest Dermatol* 97:1–8, 1991. Copyright 1991 by the Society for Investigative Dermatology, Inc.

the overlay of the screen using the cursor and the digitizing tablet. The contours are stored as a binary image, which is used as a mask (Fig. 11-5a, original image; Fig. 11-5c, original image with overlay). Before the automatic grain counting can be performed, image processing has to be carried out to improve the quality of the original image and to enhance the contrast between grains and background. This constitutes gray-value normalization and contrast enhancement by subtracting the background from the original (Fig. 11-5e). The background image (Fig. 11-5d), which seems to be out of focus, was calculated by digital filtering with a median filter of 5 × 5 pixels. Thresholding provides a binary image (Fig. 11-5g). The result of segmentation is presented in the overlay for control of the segmentation process (Fig. 11-5i). After elimination of the information outside the mask (Fig. 11-5j), the area of all grains can be summarized and the number of grains per cell can be computed using the previously determined mean area of the grains.

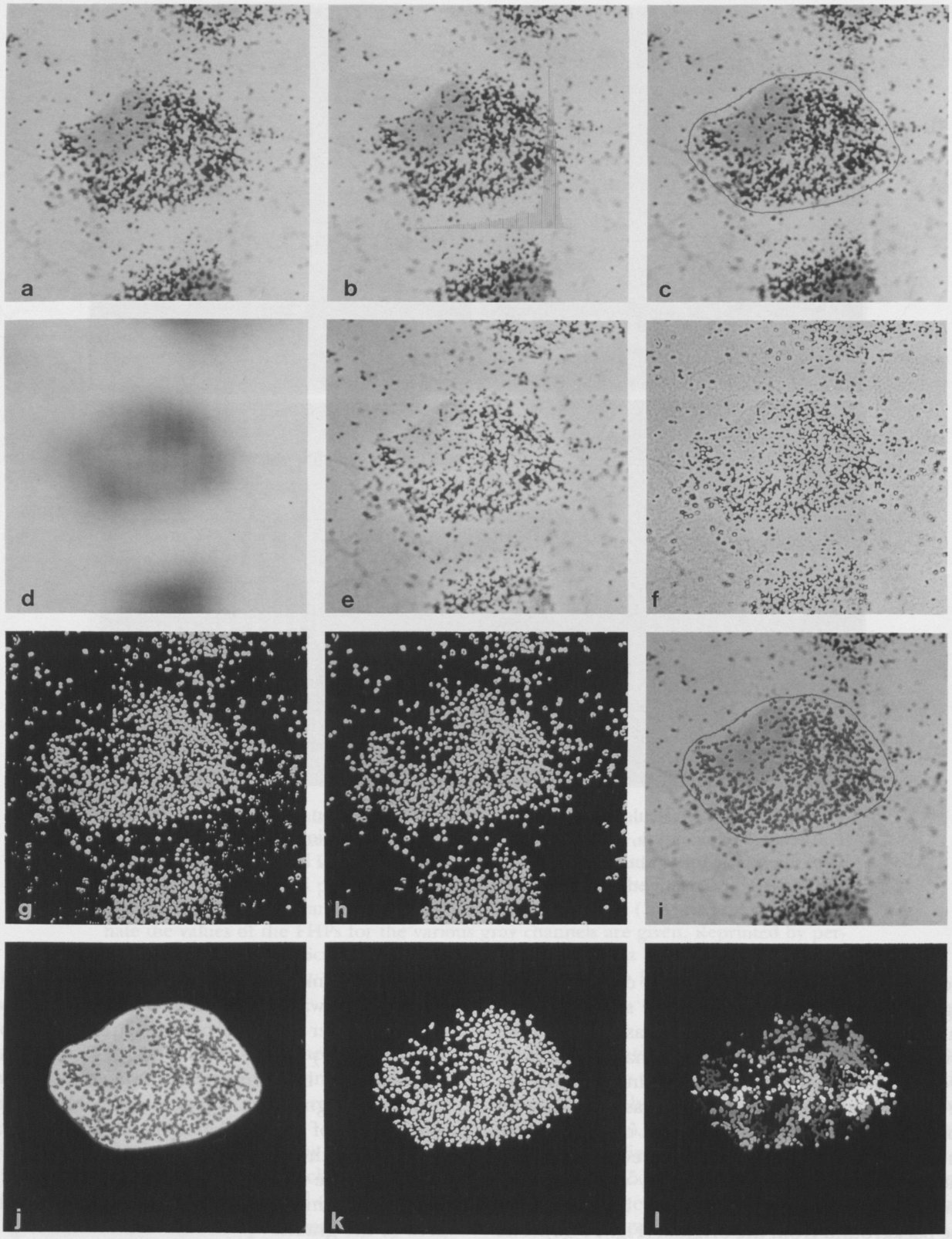
a
b
c
d
e
f
g
h
i
j
k
l

IA and three-dimensional reconstruction. Three-dimensional computer reconstruction of tissue structures based on serial sections is another important task of IA.[43] There are a large number of applications in dermatopathology, which are discussed below.

Through tissue modeling to tissue interpretation by IA. The usual approach to tumor diagnosis in dermatopathology is a heuristic approach: Qualitative and quantitative parameters of diagnostic and prognostic significance are evaluated by experience. In a new approach using computer simulation, Smolle et al. elucidated the way tumor morphology is related to the underlying biological properties of the tumor cells.[44–47]

In the learning phase of the procedure, several thousand tumor patterns were simulated by the computer, with each pattern based on different settings of the biological features. The resulting morphologic pattern in each simulation was evaluated by pattern analysis, and the resulting morphological parameters were combined with the present biological properties and evaluated by multivariate statistical analysis. The tissue-modeling procedures and the estimates derived thereof have also been validated in experiments.[44,47] In the application phase, microscopic slides of melanocytic skin tumors were fed into the computer, and the knowledge about function and morphology as derived from the learning phase was applied to estimate biological properties of the real melanocytic tumors. This approach was used for the calculation of parameters with potential prognostic significance.[46]

APPLICATIONS OF MORPHOMETRY AND DNA MEASUREMENTS

Differentiation between Malignant Melanoma and Benign Melanocytic Nevi

Morphometry. The histologic diagnosis of MM, particularly of initial MM, can be difficult, because objective, reliable, and reproducible criteria are lacking.[5,6] Several attempts have been made to establish additional objective and reliable parameters using morphometry (see Table 11-1).[47–58] Statistically significant differences between MM and melanocytic nevi (MN) were demonstrated in most studies, but the diagnostic efficiency varied between 87 and 100%. The differences might be due to different cell-sampling strategies, morphometric criteria, and instrumentation. Beside simple semiquantitative estimation and use of grids or ocular micrometers,[48,50,54–57] in the majority of cases, ICM was applied.[49,51–53,58] In nearly all studies, criteria based on nuclear area (mean; standard deviation; ratio of the means between the deep/superficial layers of a lesion, termed *maturation index*) were found to be the most useful for differentiation between MM and MN.

Fig. 11-5 Image-processing steps for the quantification of in situ hybridization (ISH). (a) Original image demonstrating alpha (I) collagen mRNA visualized by autoradiography following ISH in a fibroblast embedded in a three-dimensional gel. (b) Gray-value histogram superimposed. (c) The border of the cell was interactively determined using a cursor. (d) Calculation of a background image by applying a median filter (5 × 5 pixels). (e) Result after contrast enhancement by subtracting the background image from the original. (f) Image after further contrast enhancement by performing an addition between the original and the difference between the original image and the low-passed filtered version of it. (g) Binary image after application of a gray-value threshold (130) to the image of (f). (h) Removal of small particles, which represent segmentation artifacts not belonging to grains using a size-dependent filter. (i) Control of accuracy of segmentation. The contours of the segmented grains of (h) were given in the overlay. In addition, the mask of the cell is displayed. (j) Elimination of information outside the mask by application of the Boolean operation AND. (k) Binary image to be measured. (l) Identification of grains by the image-processing system; independent structures are indicated by different colors. Reprinted by permission of the Springer Verlag Heidelberg from Stolz et al.[42]

TABLE 11-1 Morphometric Investigations for the Differentiation between MM and Benign MN*

Authors	Methods	Technique†	Material	Cells Analyzed/ Case	Most Important Criterion	Diagnostic Accuracy (%)
Howard 1986[48]	LM	Grid	11 MN, 12 MM	50	Nuclear volume	87.0
Lindholm and Hofer 1986[49]	LM	ICM	7 MN, 83 MM, 8 N. Spitz	150	Maximum of nuclear diameter	100.0
Brüngger and Cruz-Orive 1987[50]	LM	Grid	8 MN, 8 MM	730	Nuclear volume	93.7
Stolz et al. 1987[51]	EM	ICM	10 MN, 11 MM	50	Nuclear area	100.0
Stolz et al. 1987[52]	EM	ICM	14 MN, 13 MM	50	Nuclear area	92.6
Smolle et al. 1988[53]	LM	ICM	40 MN, 40 MM, 40 N. Spitz	Not given	Maturation index‡	95.0 (MM/ MN) 97.0 (MM/ N. Spitz)
Rhodes et al. 1988[54]	EM	Semiquant.	5 DMN, 5 MN, 5 MM	8	Number of abnormal melanosomes	90.0
Olinici and Giurgiuman 1989[55]	LM	Grid	14 MN, 29 MM	50	Nuclear area	88.4
Sorensen 1989[56]	LM	Grid	62 MN, 47 MM, 14 Lentigo mal.	Not given	Volume-weighted mean nuclear volume	86.9
Leitinger et al. 1990[58]	LM	ICM	133 MN, 53 MM, 20 N. Spitz	>60	Maturation index	96.8
Stolz et al. 1991[76]	EM	Image analysis	20 MN, 17 MM	50	Number of markedly atypical nuclei (MACs)	100.0

*Abbreviations: LM = light microscopy; ICM = interactive computerized morphometry; EM = electron microscopy; DMN = dysplastic melanocytic nevus.

†Grid = grid technique according to Gundersen and Jensen;[17] Semiquant. = semiquantitative analysis.

‡Ratio of nuclear area in the superficial and deep layer of the lesion.

In a semiquantitative ultrastructural study Rhodes et al. showed that the number of abnormal melanosomes is significantly higher in MM than in MN.[54] However, only eight cells per case were analyzed, so the data should be interpreted with caution. Other investigations disclosed a progressive increase of the mean nuclear area from lentigo simplex to junctional and to dermal nevi.[59]

When ICM was used on electron microscopic sections for the measurement of the mean nuclear area (50 cells per case), 11 MM and 10 MN cases could be differentiated with an accuracy of 100%.[51] But with an increase in the number of cases analyzed, the correct classification rate decreased to 92.6%,[52] because of MMs with a mean nuclear area in the range of that of MN. In these two studies only intraepidermal melanocytes were taken into account, because Schmiegelow et al. could show that the superficial layers of MMs determine the dynamics of neoplastic growth.[60]

Olinici and Giurgiuman confirmed the importance of the nuclear area for the differentiation of MM and MN.[55] In another light microscopic study, Lindholm and Hofer reached a diagnostic accuracy of 100% by determination of the mean nuclear diameter.[49] However, the authors give no information about their sampling strategies. Smolle et al.[53] and Leitinger et al.,[58] also using ICM in light microscopy, defined the maturation index described above; when this index was used, 95%[53] and 96.8%,[58] respectively, of the melanocytic lesions were correctly classified. The efficiency of the index for identifying MM versus Spitz nevi (20 cases), which often resemble MM histologically, was

97%.[53] When the mean nuclear volumes or the volume-weighted mean nuclear volume was applied as a criterion for differentiation, which can be calculated by simple grid techniques, an efficiency of 87 to 93% was reached.[48,56,57]

DNA measurements. Since the majority of neoplasms are characterized by an increased rate of aneuploid cells,[7] DNA measurements were also applied to the differential diagnosis of melanocytic neoplasia using cytophotometry (CPM), FC, and IA for computerized DNA cytometry (CCM). Table 11-2 gives a list of the studies in chronological order. The diagnostic efficiency varies between 52 and 100% because of different methods, definitions of aneuploidy, and numbers of cases as well as different sampling strategies.

In a CPM study, Schmiegelow et al. found differences in the coefficient of variation of DNA values (ratio between mean value and standard deviation) between MM and MN.[60] Lindholm et al. were able to differentiate 17 MN, 6 Spitz nevi, and 23 MMs with an efficiency of 86.9% by CPM.[61] In this study a hyperdiploid modal value of the DNA histograms (>2.5c) was used as a discriminating criterion. When IA was applied to the detection of differences of mean DNA values between superficial and deep dermis, 84.6% accuracy was reached for the classification of MM and Spitz nevi.[62] The presence of more than 10% of the nuclei with a DNA value higher than 4c measured by CPM on imprint specimens allowed a discrimination of 89.7% of 39 cases of MM and MN.[63] A similar result with an efficiency of 89.5% was also achieved in a CCM study by Stolz and coworkers.[64] In this study three criteria were selected by multivariate statistical analysis: mean value of DNA, standard deviation of nuclear area, and the ninety-fifth percentile of the DNA histogram. Fleming et al. analyzed paraffin sections of 19 MN and 5 MMs and were able to separate all lesions using either the nuclear area or mean and standard deviation of the nuclear DNA content.[65] In addition, 24 dysplastic nevi were also investigated and showed results between those of the MMs and MN, which results were interpreted as indicative of an increased malignant potential of dysplastic nevi (see Fig. 11-6).

FC studies provided similar results with variable efficiency ranging from 69 to 100%.[34,66–74] The majority of investigators defined aneuploidy as the appearance of a distinct ploidy peak in the histogram differing more than 10% from the diploid peak and used it as a criterion for differential diagnosis of MM and MN.[66,68,70–74] Sondergaard et al.[66] and Rode et al.[75] also took polyploidy into account without significant improvement of the discriminating power.

When the results of FC and both CCM and CPM were compared, the latter techniques showed better results. This might be because in initial melanoma the rate of aneuploid cells is rather low and the capability of detecting those cells is higher in CCM and CPM than in FC.

IA for detection of both morphometric and chromatin texture features. Since in almost all studies an overlap was found between MM and MN, Stolz and Abmayr used IA for the determination of both morphometric and chromatin structure features on ultrastructural sections combined with multivariate statistics.[76] In each of 1840 intraepidermal melanocytic nuclei of 17 MM and 20 MN cases, 37 different features were determined by a Microvax 3500 computer. The classification strategy based on the identification of markedly atypical cells (MACs) MACs were defined by eight most important features, which were selected according to their F values in stepwise discriminant analysis. The most appropriate features were nuclear area; circumference; FHP 103, 118, 136, and 151; and mwdif 2 and 3. Mwdif 2 and mwdif 3 were defined as the mean gray value in the difference image between the original and the medium-filtered version of it using a filter size of 3 × 3 (mwdif 2) and 11 × 11 pixels (mwdif 3). The features selected were linearly combined into a new feature, the canonic variable (CV). When the CV was used, the grade of nuclear atypia could be quantified. The CV shows the same discriminant power as the eight features together. In Figure 11-7a the histogram of the CV values of all melanocytic nuclei analyzed is given, and in Figure 11-7b the number of MACs is presented for all MMs investigated. Markedly atypical nuclei were found in 39.4% of the MM cells, but in only 0.3% of the MN cells. The presence of MACs allowed a clear differentiation between MM and MN (see Fig. 11-7b), All MM cases exhibited more than four MACs, whereas 17 MN cases were MACs-negative, and in the remaining 3 cases only one MAC was present. Thus the rate

TABLE 11-2 Quantification of DNA Values for Differentiation between MM and Benign MN

Authors	Methods	Technique	Material	Cells Analyzed/ Case	Most Important Criterion	Accuracy (%)
Barlogie et al. 1980[34]	FC	Fresh*	120 MN, 19 MM	30,000	aneuploidy†	99.2
Sondergaard et al. 1983[66]	FC	Fresh	16 MN, 26 MM	>30,000	Aneuploidy and hyperploidy‡	69.0
Büchner et al. 1985[67]	FC	Fresh	46 MN, 721 MM	>20,000	Aneuploidy†	76.9
Von Roenn et al. 1986[68]	FC	30-μm paraffin§	34 MN, 53 MM	>10,000	Aneuploidy‡	52.8
Schmiegelow et al. 1986[60]	CPM	7.5-μm paraffin	15 MN, 9 MM	50	Coefficient of variation of DNA histogram	Not given
LeBoit and van Fletcher 1987[62]	CCM	4-μm paraffin	6 N. Spitz, 7 MM	Not given	Heterogeneity of DNA values between upper and lower dermis	84.6
Lindholm et al. 1987[61]	CPM	5-μm paraffin	17 MN, 23 MM, 6 N. Spitz	100	Hyperdiploid modal value of DNA histogram	86.9
Bergman et al. 1988[63]	CPM	Imprints	14 MN, 25 MM, 53 DMN¶	>30	>10% of the cells with 4*c* DNA or aneuploid DNA values	89.7
Newton et al. 1988[69]	FC	60-μm paraffin	44 MN, 20 DMN, 17 congenital MN	Not given	Aneuploidy†	Aneuploidy also in 6.8% of MN, 30% of DMN, and 50% of large congenital MN
Kamino and Ratech 1989[70]	FC	100-μm paraffin	22 MN, 37 MM	30,000	Number of nuclei in G_0/G_1 phase, mean value of DNA, S-100-positive subpopulations	81.3
Steijlen et al. 1989[71]	FC	40-μm cryostat sections	56 MN, 16 MM	>50,000	aneuploidy‡	Not given
Rode et al. 1990[75]	CCM	Paraffin	16 MN, 19 MM, 35 N. Spitz	200	poly-, and hyperdiploidy	Not given
Fleming et al. 1990[65]	CCM	6-μm paraffin	19 MN, 5 MM, 24 DMN	100	Standard deviation of nuclear area, mean value or standard deviation of DNA histogram	89–100
Chi et al. 1990[72]	FC	50-μm paraffin	20 MN, 20 MM, 20 N. Spitz	>100	Mean DNA value	100

TABLE 11-2 continued

Authors	Methods	Technique	Material	Cells Analyzed/ Case	Most Important Criterion	Accuracy (%)
Slater et al. 1991[73]	FC	50-μm paraffin	18 MN, 16 MM, 40 DMN	>10,000	Aneuploidy‡	75
	CCM	Imprints	18 MN, 39 MM	100	Mean value and standard deviation of DNA histogram, 95th percentile of the DNA histogram	89.5
Sangueza et al. 1992[74]	FC	50-μm paraffin	43 MM, 16 MN, 11 N. Spitz, 15 DMN	>30,000	Aneuploidy‡	62.8
Stolz et al. 1993[64]	CCM			100		71.4

*Fresh tissue was used for preparation.

†No accurate definition was given.

‡Aneuploidy is stated, if an additional peak appears in DNA histogram located more than 10% from the 2*c* value, hyperploidy if in more than 15% of the nuclei, DNA exceeds 4*c*.

§Paraffin sections.

¶DMN = dysplastic melanocytic nevus.

of correct classification was 100% if an adequate threshold was set.

Figures 11-8a and 11-8b demonstrate the differences in chromatin structure between MN cells (Fig. 11-8a) and MACs (Fig. 11-8b).

In a recent study the identical strategy could also be applied to light microscopic semithin sections. By the presence of MACs, 27 MM and 21 MN cases could be differentiated with an efficiency of 94%.[77]

Prognostic Significance of Morphometry and DNA Measurements in MM

Morphometry There are numerous studies investigating the use of morphometry for the prognostic evaluation of MM (see Table 11-3).[56,78–85]

Sorensen et al. used grid techniques to define the mean volume-weighted nuclear volume and found that this was a valuable and objective prog-

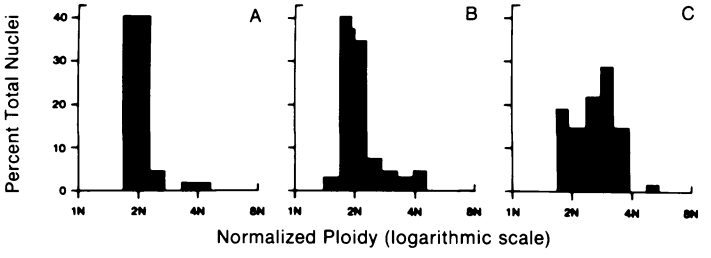

Fig. 11-6 Mean value of DNA content in common MN, (A) dysplastic nevi, (B) and melanomas. Reprinted by permission of the Elsevier Science Publishing Co., Inc. from Fleming et al.[65] Copyright 1990 by the Society for Investigative Dermatology, Inc.

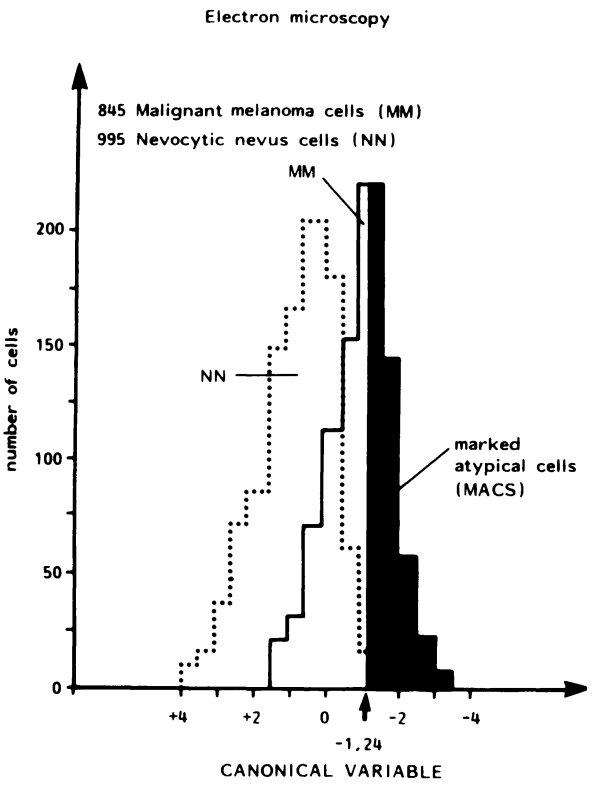

a

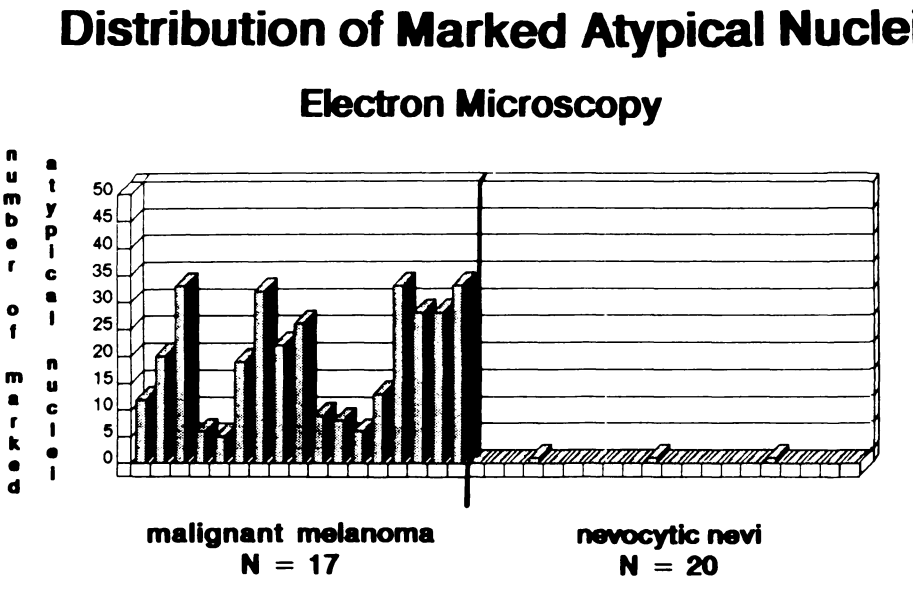

b

Fig. 11-7 (a) Histogram of CVs in MMs and MN. Multivariate cell classification, electron microscopy. Black column: localization of the MACs, CV < -1.24. (b) Distribution of MACs within cases investigated by electron microscopy. None of the benign MN contained more than one MAC, whereas in all MMs analyzed, more than four MACs were present. (a) and (b) reprinted by permission of the Elsevier Science Publishing Co., Inc. from Stolz et al, *J Invest Dermatol* 97:1–8, 1991. Copyright 1991 by the Society for Investigative Dermatology, Inc.

nostic marker in MM.[56,57] The majority of the remaining investigators used ICM. In the studies of Tan and Baak the correlation coefficient of nuclear area and perimeter reached the prognostic significance of tumor thickness, which was found to be the most valuable indicator for survival in many prospective studies.[78,79] Lindholm et al. found nuclear diameter and tumor thickness to be the best predictors of clinical outcome.[79] Srivastava et al. analyzed vascularization of MMs and found an increased area of vascular sections in metastasizing MM compared with nonmetastasizing tumors, especially in MM thinner than 0.75 and thicker than 3 mm.[81]

In ocular MM the morphometric constituents of the nucleoli turned out to be significantly correlated with the risk of invasion of orbital tissues; metastases; and survival time.[80,82,83]

DNA measurements. As presented in Table 11-4, a considerable number of investigations provide FC data for the prognostic evaluation of MM.[66,68,86–100] Hansson et al.[86] and Frankfurt et al.[87] measured the rate of S-phase cells, showing lower survival probability if the rate is higher than 10% of the cells analyzed. In addition, a significant correlation between the appearance of aneuploid peaks (defined as differing more than 10% from the diploid value) and other prognostic features such as tumor thickness and depth of invasion was demonstrated.[66] Kheir et al. found aneuploidy to be an independent prognostic marker in stage I MM <1.5 mm and >3 mm thick.[88]

Aneuploidy also proved to be a good predictor of recurrence.[68] Bines et al. investigated 177 cases of MM, and aneuploidy turned out to be the most significant prognostic factor after thickness adjustment.[89] Also an acceleration in the generation of new aneuploid cell lines was found in patients dying from metastatic MM.[90]

However, there are some contradictory results, showing no significant association of aneuploidy and time of survival,[91,92] especially if data were stratified according to tumor thickness. In the study of Gattuso et al., aneuploidy was related to shorter survival but lost its significance after thickness stratification.[93]

Also, CPM and CCM data are available. The variation of the DNA values around the diploid peak was found to influence survival independently of tumor thickness and age.[94] Feulgen-stained imprint specimens were used by Vogt et al.[95] The CCM data showed a significant correlation between DNA indices (mean DNA value, mean $2c$ deviation index, $5c$ exceeding rate) and tumor thickness. In contrast, Lindholm et al., found no correlation between DNA modal value and prognosis.[96] Zeng et al. analyzed 22 metastases by IA and found significant correlations among low survival time and increased variation in DNA values and the presence of multiple clonality.[97] Aneuploidy of MM in situ adjacent to nodular MM was described by Schmiegelow et al. using CPM.[98] Further studies are necessary to establish the full benefit of CPM and CCM for the prognostic evaluation of MM.

Malignant Non-Hodgkin's Lymphomas of the Skin

Differentiation between malignant lymphomas and pseudolymphomas of the skin. The difficulties in the differential diagnosis of malignant lymphoma (ML) and pseudolymphoma (PL) arise from the poorly defined histologic criteria.[101] If rules are devised to differentiate between ML and PL, exceptions to these rules abound.[102] To obtain more precise and objective dignostic criteria, several techniques were used, for example, quantitative electron microscopy,[103] FC,[104] and DNA CPM.[105]

Immunophenotyping has been shown to be inconclusive, particularly in T-cell infiltrates, and further experience must be gained with this modality.[101,102]

Van Vloten et al. provided DNA CPM data for the differentiation of ML and PL.[101,102] However, in their study only a rough evaluation of the DNA histograms was performed. Thus the sensitivity of the method applied was only 75%.

In a recent study we used high-resolution CCM for the differential diagnosis of ML and PL. The most important result was that the efficiency, sensitivity, and specificity of the $2c$ deviation index ($2c$DI) was 94%.[107] The $2c$DI is defined according to Böcking as the ratio between the sum of the squares of the differences between the DNA values of individual cells, c_i, and the normal diploid DNA value $2c$, and the number of cells measured, N:[108]

$$2c\text{DI} = \frac{1}{N}\sum_{i=1}^{N}(C_i - 2c)^2$$

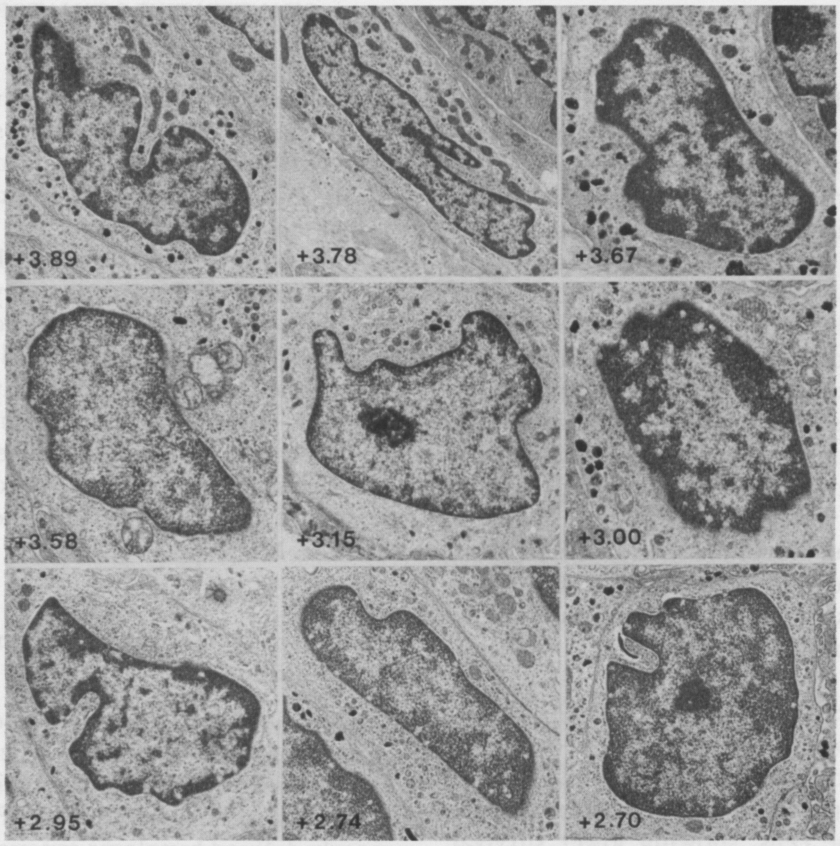
+3.89
+3.78
+3.67
+3.58
+3.15
+3.00
+2.95
+2.74
+2.70

a

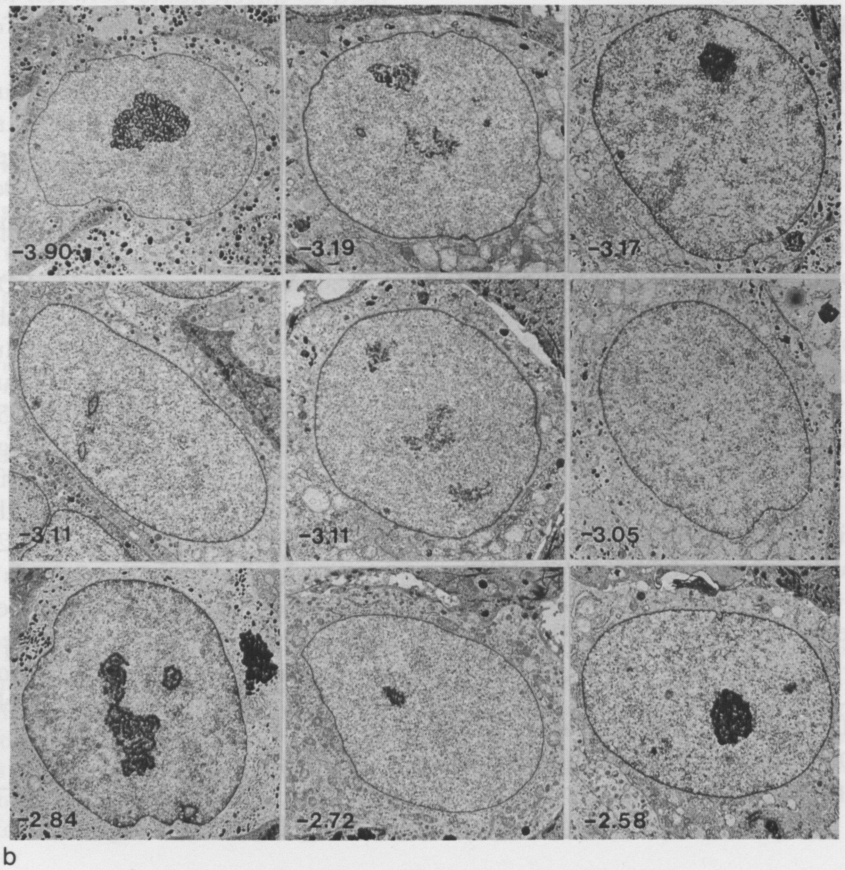
-3.90
-3.19
-3.17
-3.11
-3.11
-3.05
-2.84
-2.72
-2.58

b

TABLE 11-3 Prognostic Significance of Morphometry in Cutaneous and Ocular (*) MM

Authors	Method†	Technique	Number of Cases	Cells/Case	Result
Gebhard and Knobler 1984[84]	LM	ICM	3	Not given	Three-dimensional reconstruction of tumor volume does not improve prognostic evaluation.
Tan and Baak 1984[78]	LM	ICM	68	50	Tumor thickness, variation coefficient of nuclear perimeter, and area are the best prognostic criteria.
Srivastava et al. 1988[81]	LM	ICM	20	3–18 object fields (×40)	Area of vascular spaces is significantly larger in metastasizing than in nonmetastasizing melanomas.
Lindholm et al. 1988[79]	LM	ICM	82	150	Tumor thickness and largest nuclear diameter are the best prognostic criteria.
Sorensen 1989[56]	LM	Grid‡	47	Not given	Volume-weighted mean nuclear volume is the most important prognostic criterion.
Gamel and McLean 1983[80]	LM	ICM	150*	200	Inverse standard deviation of nucleolar perimeter and tumor thickness are the most important prognostic criteria.
Gamel et al. 1986[82]	LM	ICM	540*	200	Inverse standard deviation of nucleolar area correlates with 5-year survival rate.
Donoso et al. 1986[85]	LM	ICM	30*	200	Inverse standard deviation of nucleolar area is the most appropriate predictor of survival.
Tosi et al 1987[83]	LM	ICM	15*	50	Nuclear area and nucleolar area differ significantly between choroidea infiltrating and noninfiltrating ocular melanoma.
Sorensen et al. 1991[57]	LM	Grid‡	56	Not given	Poor correlation between volume-weighted mean nuclear volume (VV) and DNA content determined by FC; in Cox model only VV was an independent prognostic variable.

†LM = light microscopy.

‡Grid technique according to Gundersen and Jensen.[17]

Fig. 11-8 Ultrastructural micrographs of melanocytic nuclei of (a) MN and (b) MMs, which present the characteristic differences in chromatin structure. The MACs from MM contain more euchromatin and fewer dark chromatin aggregates outside the nucleolus compared with cells from MN. The morphologic differences are reflected by opposite CVs, which are given in the lower left corner of each nucleus. The MACs (b) show CVs between −3.9 and −2.58, whereas the benign nuclei (a) are characterized by values between +2.7 and +3.89. Reprinted by permission of the Elsevier Science Publishing Co., Inc. from Stolz W et al, *J Invest Dermatol* 97:1–8, 1991. Copyright 1991 by the Society for Investigative Dermatology, Inc.

TABLE 11-4 Prognostic Significance of DNA Measurements in Cutaneous and Ocular (*) MM

Authors	Method	Technique	Number of Cases	Cells/Case	Result
Hansson et al. 1982[86]	FC	Fine needle biopsy	38 metastases	>10,000	Significant decrease of survival time in cases with an increased (>10%) rate of S-phase cells.
Sondergaard et al. 1983[66]	FC	Fresh†	26	>10,000	Aneuploidy and high 4*c* peaks are more frequent in tumors >2.25 mm.
Frankfurt et al. 1984[87]	FC	Fresh	61	50,000	Aneuploidy and increase of S-phase cells is associated with shorter survival
Von Roenn et al. 1986[68]	FC	30-μm paraffin‡	53	>10,000	90% of the aneuploid MM were recurrent; in the diploid cases this rate was only 17% ($p < .0005$).
Schmiegelow et al. 1987[98]	CPM	7.5-cm paraffin	10 (in situ)	Not given	DNA histograms indicate the malignant potential of MM in situ adjacent to invasive nodular MM.
Kheir et al. 1988[88]	FC	50-μm paraffin	162	10,000	Aneuploidy is correlated with tumor thickness and depth of invasion; aneuploidy is an independent prognostic marker in MM <1.5 and >3 mm.
Zaloudik et al. 1988[91]	FC	30-μm paraffin	50	5000	No significant correlation between aneuploidy and time of survival.
Bines et al. 1988[89]	FC	50-μm paraffin	177	50,000	Aneuploidy is the most significant prognostic factor after thickness adjustment.
Heenan et al. 1989[94]	CCM	5-μm paraffin	97	200	Deviation from diploidy influences survival, but tumor thickness is a better prognostic criterion.
Lindholm et al. 1990[96]	CCM	5-μm paraffin	50	100	Modal values of DNA histograms are not significantly correlated with prognosis and tumor thickness.
Zeng et al. 1990[97]	CCM	10-μm paraffin	22	>250	Poor survival rate is associated with multiple clones and increased coefficient of variation of DNA content.
Gattuso et al. 1990[93]	FC	50-μm paraffin	55	10,000	DNA aneuploidy was significantly correlated with disease-free survival and poorer prognosis, but lost its impact if data was stratified for tumor thickness.
Rode et al. 1991[92]	FC	5-μm paraffin	52	200	DNA distribution and aneuploidy are not reliable for prediction of metastases.
Bartkowiak et al. 1991[90]	FC	Fresh	73	Not given	Correlation between prognosis and rate of S-phase cells, aneuploidy, and multiclonality.
Ohnishi and Ishikawa 1991[99]	FC	30-μm paraffin	28	>10,000	Aneuploidy more frequent in thicker tumors.
Björnhagen et al. 1991[100]	CPM	4-μm paraffin	28	100	In tumors >3 mm, more than 3% 5*c* nuclei is correlated with unfavorable prognosis.
Vogt et al. 1993[95]	CCM	Imprints	34	100	Significant correlation between DNA indices and tumor thickness.

† Fresh tissue was used for preparation.

‡ Paraffin sections.

Roughly, the 2*c*DI reflects the variation in the nuclear DNA values around the 2*c* value within one case. The values for the individual cases studied are given in Figure 11-9.

The sensitivity of the 2*c*DI was higher than in previous investigations, in which CPM was used on skin imprint specimens both for the differentiation between ML and PL[106] (sensitivity 75%) and for the diagnosis of cutaneous T-cell lymphomas[109,110] (sensitivity 65 and 50%, respectively). In those studies the percentage of cells having a DNA content higher than 4*c* (4*c* exceeding rate, 4*c*ER) or a content of more than 4*c* + 2SD (SD = standard deviation) of the mean DNA value was used as a discriminating feature. Applying the 4*c*ER in our series, we found similar results with a sensitivity of 62% and a specificity of 94%.[107] In contrast to the 4*c*ER, the 2*c*DI is already increased if cells with a DNA content between 2.25*c* and 3.5*c* are present. Such cells are either aneuploid or normal proliferating cells within the S phase. Their relevance was not considered in previous CPM studies.[106,109,110] Four typical, different patterns of DNA histograms of ML and PL were found (Figure 11-10a to 11-10d), as was also reported in a CPM study of lymph node touch imprints in cutaneous T-cell lymphomas.[111] A pattern similar to that of Figure 11-10d was exclusively found in lymph nodes with focal or diffuse infiltration with ML cells.

DNA measurements in lymphomatoid papulosis (LP) type A were inconclusive. In our data, one of two cases showed a 2*c*DI higher than 0.1, which is usually found in ML. Our data is consistent with the evaluation of 13 cases of LP using FC,[112] in which markedly abnormal DNA values could be demonstrated in only 2 out of 13 patients, but

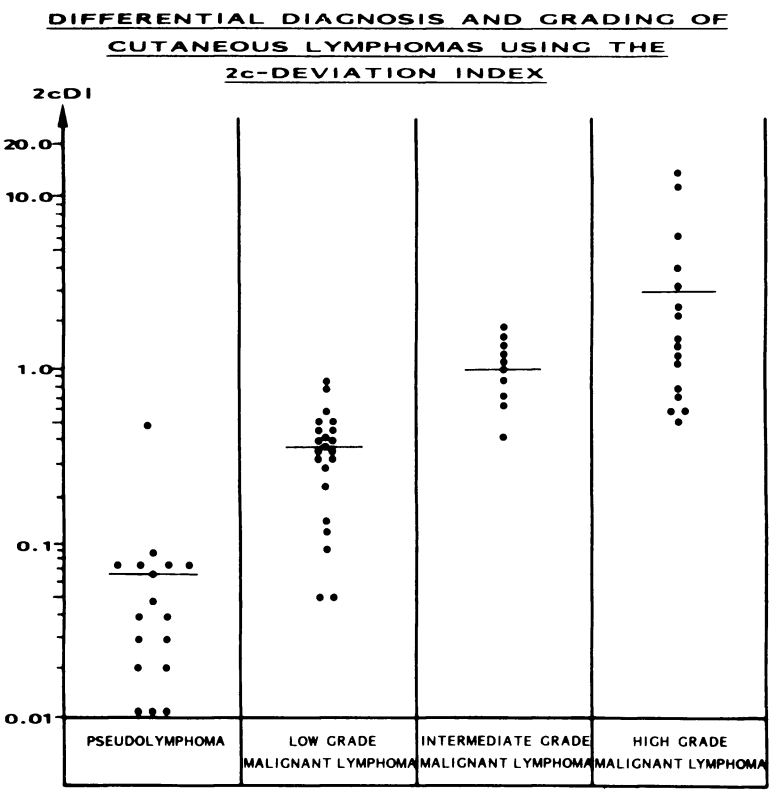

Fig. 11-9 Using a 2*c*DI > 0.1 as marker for MLs, 16 of 17 cases of PL and 46 of 49 cases of ML were correctly classified. The three false-negative cases were of low-grade malignancy. The 2*c*DI also allows a significant discrimination between low-grade, intermediate-grade, and high-grade MLs.

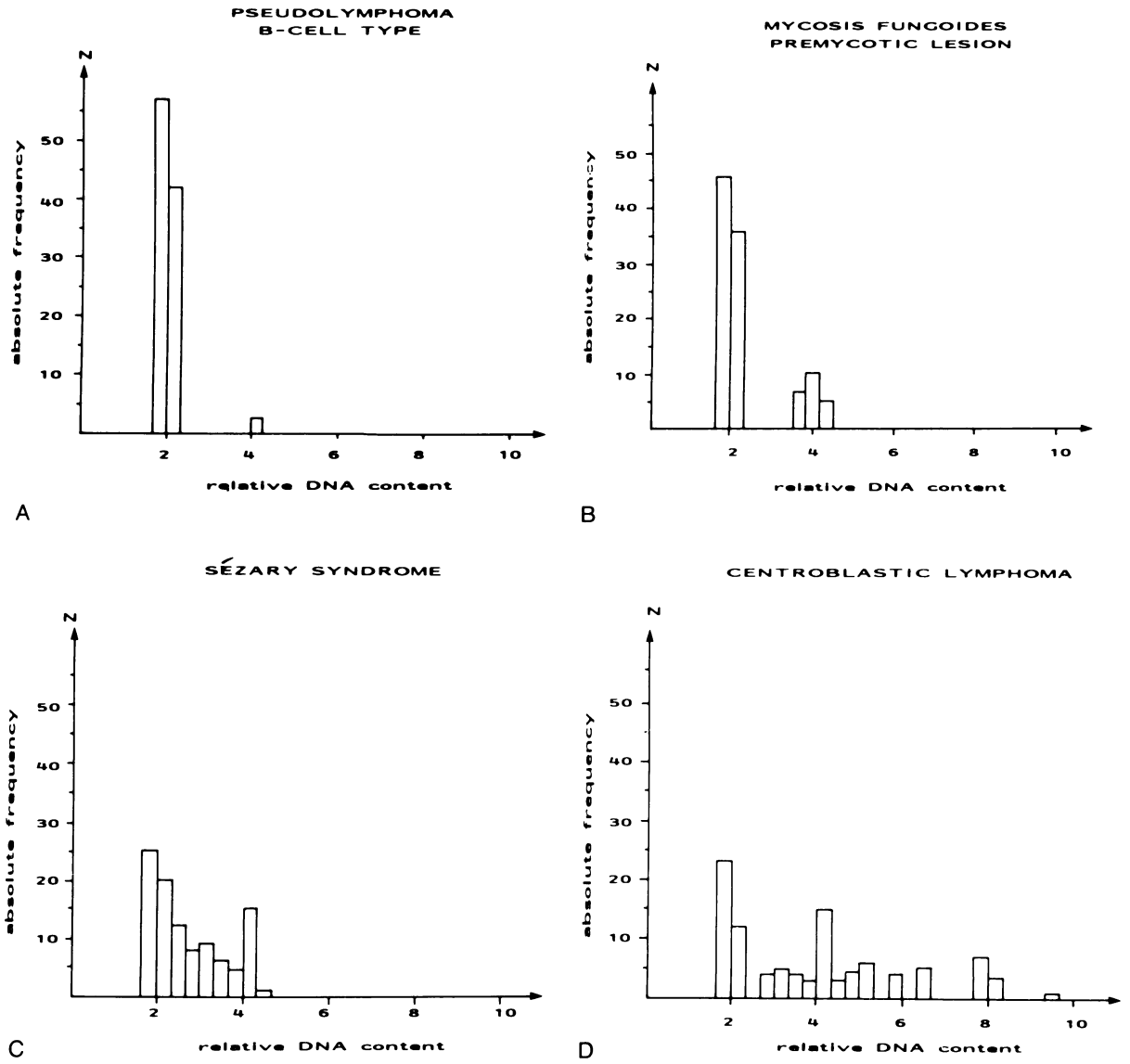

Fig. 11-10 Characteristic patterns of DNA histograms. (a) PL. Cells with a DNA content higher than 5*c* were not detected, and also a gap between 2.25 and 3.5*c* was present. (b) An intermediate type of histogram with a 4*c* peak higher than 5%. (c) and (d) Histograms of MLs. Histograms resembling (c) lack a gap between 2.25 and 3.5*c* DNA; histograms similar to (d) show cells with a DNA content of more than 5*c*. Reprinted by permission of the Elsevier Science Publishing Co., Inc. from Stolz et al.[107] Copyright 1990 by the Society for Investigative Dermatology, Inc.

are in contrast to data of Willemze et al.[113] They found abnormal DNA histograms in all cases of LP type A.

FC studies revealed that a hyperdiploid peak might be of diagnostic importance in ML,[114] but such findings were also demonstrated in PL and in positive patch test lesions.[115] Joensuu et al. performed DNA FC combined with fine needle aspiration biopsies for the differentiation between nodular ML and PL.[116] True aneuploidy was demonstrated in 11 out of 35 ML cases. However, if the number of proliferative cells, a feature similar to the 2*c*DI, was taken into account, the diagnostic efficiency increased to 81%. Also, Pastel-Levy et al. could find aneuploid cells by FC in only 27% of tissues from mycosis fungoides.[117]

High-resolution IA offers the opportunity to study both DNA content and chromatin structure, as was reported for lymphoid blood cells of patients with cutaneous T-cell lymphoma.[118] Since abnormalities in the chromatin structure may precede quantitative DNA changes,[119] further insights in the field of ML can be expected from IA of ML.[120,121]

Prognostic significance of DNA measurements in cutaneous ML. The correct grading of skin infiltrates in ML is an important prerequisite for the selection of the most appropriate therapy. At present, morphologic classification systems, such as the Kiel classification[122] allow only a rough discrimination between low- and high-grade ML, which does not reflect the full range of biological variation. Grading of ML according to morphologic features is subjective and has been proved to be not sufficiently reproducible.[123] Moreover, about 15% of MLs do not fit into common classification schemes.[124] It was demonstrated by Kerl et al. that morphologically defined subgroups can still also be heterogenous.[125] His study demonstrated that in mycosis fungoides (MF), four relevant prognostic subgroups can be identified by semiquantitative histology and that some cases have the same poor prognosis as high-grade lymphomas. Beyond histology, more objective and reliable criteria are needed for an accurate prognostic assessment of individual ML lesions.

We examined the prognostic impact of CCM on imprint specimens of ML and its relation to histologic grading.[126] The 2*c*DI allowed a significant discrimination between low-, intermediate-, and high-grade ML applying a modified Kiel classification ($p < .05$, two-sided U test, see Figure 11-9). The 4*c*ER was not able to discriminate between intermediate- and high-grade ML, and the zone of overlap between the groups was larger than when using the 2*c*DI. The 5*c*ER, giving the number of nuclei with more than 5*c* DNA and therefore being an indicator for definite aneuploidy, was not reliable enough for grading. This criterion seems to be more efficient for the differential diagnosis between benign and malignant lesions.[107]

The relevance of the 2*c*DI was confirmed by its clinical impact. The association of the $\log_{10}(2c\text{DI} + 1)$ and the logarithm of the time (number of months) elapsed until the next-higher TNM stage was reached, or a lethal outcome occurred, was significant ($p < .05$) (see Fig. 11-11). This was also true within the low-grade group alone, indicating a heterogenous prognosis within a morphologically defined subgroup and stressing the advantage of the 2*c*DI for prognostic evaluation. In the group of low-grade ML cases, the 5*c*ER was always lower than 5%; thus the benefit of using the 2*c*DI was not based on the presence of numerous aneuploid nuclei with DNA values higher than 5*c*, but on the relative increase in the number of cells with a DNA content between 2.25 and 3.5*c* DNA. For high-grade ML, the association was not significant, which might be due to the low number of cases in this subset. When the regression line in Figure 11-11 is used, the individual risks of the patients can be determined more precisely than by a rough discrimination between low-, intermediate, and high-grade ML.

Morphometry in Experimental Dermatology

There are numerous aspects of dermatologic research in which objective quantification is suitable. In many cases nonmorphologic quantification (biochemical, immunochemical, and molecular biological) is required, but morphologic quantification can also be very helpful, as was shown by Smolle et al.[127]

Other Applications

Herzberg et al. used CCM for the differentiation of keratoacanthoma (KA) and squamous cell carci-

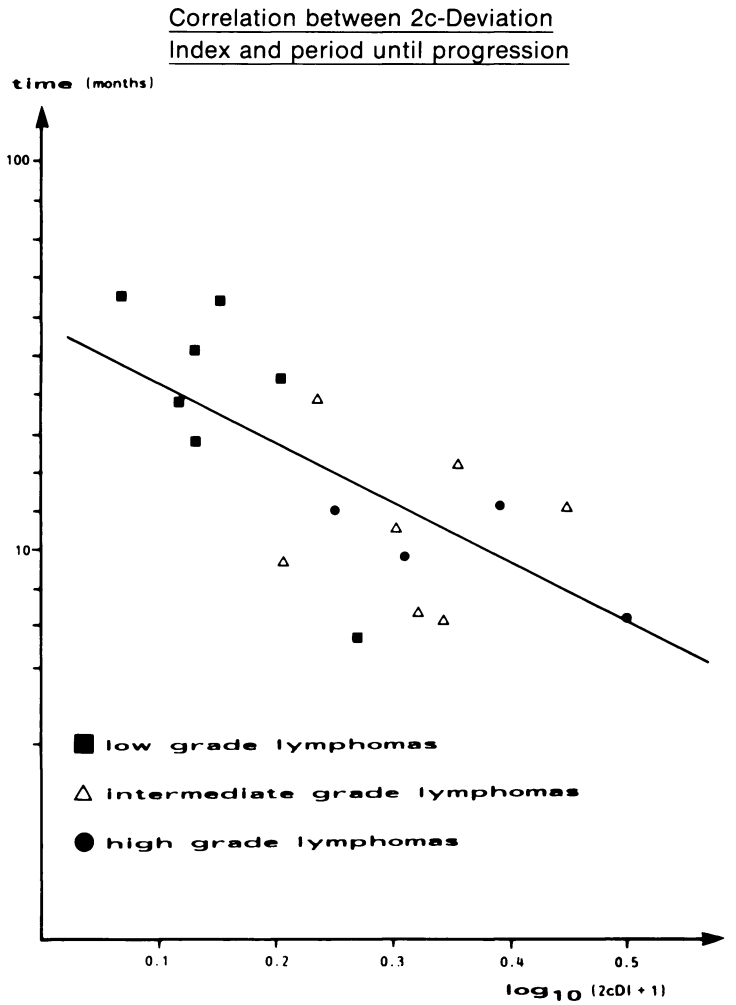

Fig. 11-11 Significant correlation between 2*c*DI and prognosis in cutaneous MLs. Reprinted by permission of the J. B. Lippincott Company from Vogt et al.[126]

noma (SCC) in paraffin-embedded tissue sections.[128] A DNA index >1.09 (ratio of the main DNA peak and the 2*c* standard) discriminated KA and SCC in 17 of 22 cases ($p < .0007$).

Recently, because of the tremendous increase in the number of patients with acquired immunodeficiency syndrome (AIDS), DNA analysis has also been used to elucidate the nature of Kaposi sarcoma (KS).[129,130] Since most of the cells appeared to be diploid, it was stated that KS is primarily an inflammatory disease, and the lack of immune surveillance is most probably responsible for its progression in AIDS patients.[129] When CCM was used, the DNA values differed significantly between initial or plaque lesions and tumor lesions. In addition, it could be demonstrated that angiosarcoma (four cases) and dermatofibrosarcoma protuberans (five cases) had significantly higher DNA values than initial and plaque lesions of KS.[130]

IA techniques also provide very useful tools for three-dimensional reconstruction of objects from serial sections. For this purpose Braverman's group designed a microcomputer graphics system with a Motorola 68000 CPU running with the Unix operating system.[43] The application of this system gave insight into the morphology of endothelial gaps in psoriatic vessels, which appeared to be identical with gaps provoked by the intradermal

injection of histamine.[131] Those gaps often contain cytoplasmatic processes, suggesting that gap formation is induced rather by cellular injury than by a pure physiologic reversible phenomenon.[131] Another study elucidated the endothelial-pericyte relationship in diabetic cutaneous vessels,[132] offering an explanation for the known increased vascular permeability in diabetes and for the development of diabetic retinopathy with aneurysm formation (see Fig. 11-12). In other studies human hair form,[133] the pathogenesis of monilethrix,[134] and human Langerhans cells were investigated.[135] Reconstruction of intradermal and epidermal tumors, for example, basal cell carcinoma[136] and MN,[137] might complete our three-dimensional perception of lesions, which usually appear two-dimensional to dermatopathologists.

FUTURE DEVELOPMENTS

The high end of computer applications as diagnostic and prognostic tools is the development of expert systems and neural networks. Expert systems are able to integrate the results of quantitative measurements with a diversity of information provided by a database.[138] In addition they can interact with a user, requesting certain answers and dispensing advise, and suggesting decisions exactly as a human consultant would. Furthermore some artificial intelligence systems have learning capabilities. These systems generalize on the base of examples and may be able to construct complex decision structures and keep them updated. Expert systems should also select the optimum procedures and control the flow of different information until a final diagnosis can be made.[12] One of the newer and very exciting artificial intelligence approaches to the development of expert systems for diagnostic purposes is the artificial neural network, or simulated parallel distributed processing. These techniques are inspired by their biological neural analogs. The networks use individual processing elements, which are highly interconnected, and which embody their knowledge through the strength of their interconnections. They allow a multiple perspective approach, which is required for the visual analysis of cell and tissue specimens. Although the rule-based system has the advantage of allowing human understanding, learning capacity and the higher diagnostic capabilities of the

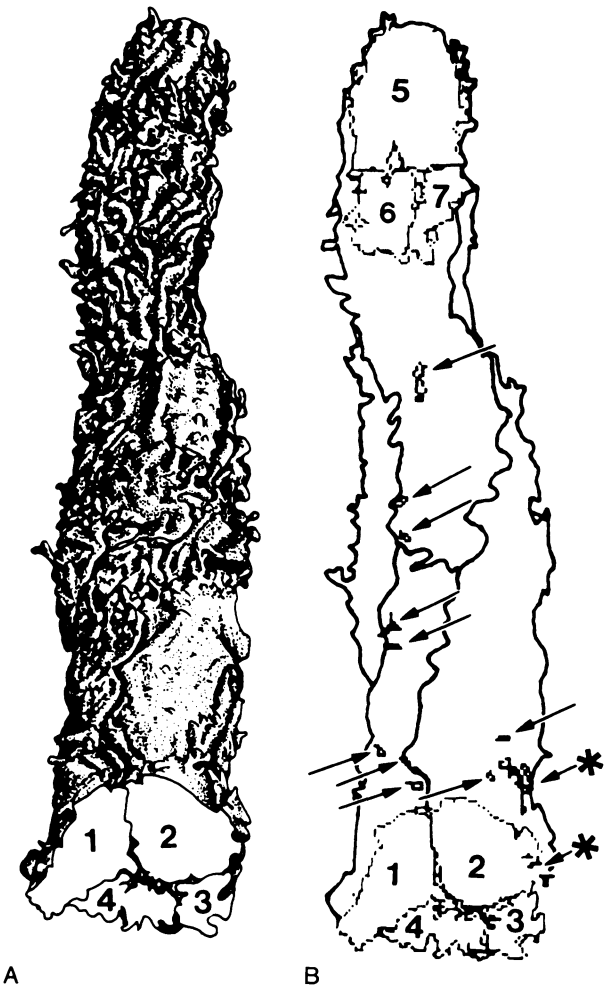

Fig. 11-12 (a) Three-dimensional reconstruction of endothelial cell tube in a diabetic postcapillary venule demonstrating rugose abluminal surface produced by elongated cytoplasmic processes that make contact with pericytes. Numbers 1 to 4 are the outlines of the endothelial cells in the last serial section of the reconstruction (130 μm long). (b) Same reconstruction as (a). Only first serial section (cells 5 to 7) and last serial section (cells 1 to 4) are shown. Graphics program reconstructs sections from top to bottom. Boundaries of endothelial cells are outlined by solid lines. Arrows indicate sites of gap formations. Arrows with asterisks indicate sites where there are clusters of three gaps. Reprinted by permission of the Elsevier Science Publishing Co., Inc. from Braverman et al.[132] Copyright 1990 by the Society for Investigative Dermatology, Inc.

nonlinear, implicit artificial neural networks give them the overall advantage. Wied and coworkers have employed several multilayer neural network models for the evaluation of objective cytometric and histiometric data.[12] Particularly, the association between DNA hitogram data and specific diagnostic categories through the use of multilayer feedforward nets trained by means of a backpropagation algorithm has proved to be very encouraging. Within Blois's paradigm (Chapter 1), the use of the computer within dermatology has the greatest potential within the specialized data-rich domain of dermatopathology.

REFERENCES

1. Lebert H: *Traité pratique des maladies cancreuses et des affections curables confondues avec le cancer.* Paris, Bailliere, 1851.
2. Virchow R: *Die krankhaften Geschwülste.* Berlin, Hirschwald, 1863–1867.
3. Cowdry EV: Results secured by applying the Feulgen reaction to fibroblasts and sarcomatous cells in tissue cultures. *Science* 68:138–140, 1928.
4. Feulgen R, Rossenbeck H: Mikroskopisch-chemischer Nachweis einer Nucleinsäure vom Typ der Thymonucleinsäure und die darauf beruhende elektive Färbung von Zellkernen in mikroskopischen Präparaten. *Z Physiol Chem* 135:203–248, 1924.
5. Jones RE: What are your five most important histological criteria for the diagnosis of malignant melanoma? *Am J Dermatopathol* 6:337–339, 1984.
6. Schmoeckel C: How consistent are dermatopathologists in reading early malignant melanoma and lesions precursor to them? An international survey. *Am J Dermatopathol* 6 (suppl):13–24, 1983.
7. Hall TJ, Fu YS: Applications of quantitative microscopy in tumor pathology. *Lab Invest* 53:5–21, 1985.
8. Baak JPA, Oort J: *A Manual of Morphometry in Diagnostic Pathology.* Berlin, Springer, 1983.
9. Weibel ER: *Stereological Methods,* vol. 1, *Practical Methods for Biological Morphometry.* London, Academic Press, 1979.
10. Auer G, Askensten U, Ahrens O: Cytophotometry. *Human Pathol* 20:518–527, 1989.
11. Koss LG, Czerniak B, Herz F, Wersto RP: Flow cytometric measurements of DNA and other cell components in human tumors: A critical apprisal. *Hum Pathol* 20:528–548, 1989.
12. Wied GL, Bartels PH, Bibbo M, Dytch HE: Image analysis in quantitative cyto-histopathology. *Hum Pathol* 20:549–571, 1989.
13. Dytch HE, Bibbo M, Puls JH, Bartels PH, Wied GL: Software design for an inexpansive, practical, microcomputer-based DNA cytometry system. *Anal Quant Cytol Histol* 8–18, 1985.
14. Williams RA, Rode J, Dhillon AP, Jarvis LR, Skinner JM, Jamal O: Measuring S100 protein and neurone specific enolase in melanocytic tumours using video image analysis. *J Clin Pathol* 39:1096–1098, 1986.
15. Van Neste DJJ, Staquet M-J, Leroy BP, De Coster WJ: Distribution pattern of psoriatic keratoblasts: Computer-assisted image-analysis for combined evaluation of DNA synthesis and expression of 67 Kilo Dalton keratin polypeptides in the epidermis of stable plaques of psoriasis. *J Invest Dermatol* 90: 382–386, 1988.
16. Marchewsky AM, Gil J, Jeanty H: Computerized interactive morphometry in pathology: Current instrumentation and methods. *Hum Pathol* 18:320–331, 1987.
17. Gundersen HJG, Jensen EB: Stereological estimation of the mean volume-weighted mean volume of arbitrary particles observed on random sections. *J Microsc* 138:127–142, 1985.
18. Jagoe R, Sowter S, Slavin G: Shape and texture analysis of liver cell nuclei in hepatomas by computer aided microscopy. *J Clin Pathol* 37:755–762, 1984.
19. Atkin NB, Richards BM: Desoxyribonucleic acid in human tumours as measured by microspectrophotometry of Feulgen stain: A comparison of tumours arising at different sites. *Br J Cancer* 10:769–786, 1956.
20. Böhm N, Sandritter W: DNA in human tumors. A cytophotometric study. *Curr Top Pathol* 60:152–219, 1975.
21. Bibbo M, Bartels PH, Dytch HE, Wied GL: Ploidy measurements by high resolution cytometry. *Anal Quant Cytol Histol* 7:81–87, 1985.
22. Van der Ploeg M, Van der Broek K, Smeulders AWM, Vossepoel AM, Van Duijn P: HIDACSYS: Computer programs for interactive scanning cytophotometry. *Histochemistry* 54:273–288, 1977.
23. Wied GL, Bartels PH, Bahr GF, Oldfield DG: Taxonomic intracellular analytic system (TICAS) for cell identification. *Acta Cytol* 12:180–204, 1968.
24. Kint A: Histophotometric investigation of the nuclear DNA-content in normal epidermis, seborrheic keratosis, keratosis senilis, squamous cell carcinoma and basal cell carcinoma. *J Invest Dermatol* 40:95–100, 1963.
25. Ehlers G: Vergleichende quantitativ-cytochem-

ische Untersuchungen über den Desoxyribonucleinsäure und Nucleohistongehalt von Basalzellepitheliomen. *Arch Klin Exp Dermatol* 232: 102–118, 1968.
26. Manocha SL: The diploid desoxyribonucleic acid (DNA) content of basal cell carcinomas in man. *Experientia* 25:201–203, 1969.
27. Ehlers G, Herbstreit A, Kampffmeyer U: Klinische, histologische und zytophotometrische Untersuchungen über primär kutane, metastatisierende, angioblastische Reticulosarkome unter besonderer Berücksichtigung der Wirksamkeit von Zytostatika. *Hautarzt* 22:245–252, 1971.
28. Ehlers G: Quantitativ histochemische Untersuchungen über den Desoxyribonucleinsäure-, Histon- und Gesamtproteingehalt in Zellkernen maligner Melanome. *Arch Klin Exp Dermatol* 237: 283–287, 1970.
29. Bloch DP, Goodman GC: A cytological and cytochemical investigation of the development of the viral papilloma of human skin. *J Exp Med* 105:161–176, 1957.
30. Kamentsky LA, Derman H, Melamed MR: Ultraviolet absorption of epidermoid cancer cells. *Science* 142:1580–1583, 1963.
31. Kamentsky LA, Melamed MR: Spectrophotometric cell sorter. *Science* 156:1364–1365, 1967.
32. Johnson TS, Katz RL, Pershouse M: Flow cytometric applications in cytopathology. *Anal Quant Cytol Histol* 10:432–458, 1988.
33. Mayall BH: Cytometry in the clinical laboratory: Quo vadis? *Ann NY Acad Sci* 468:1–18, 1986.
34. Barlogie B, Drewinko B, Scumann J, et al: Cellular DNA content as a marker of neoplasia in man. *Am J Med* 69:195–203, 1980.
35. Lovett EJ, Schnitzer B, Keren DF, Flint A, Hudson JL, McClatchey KD: Application of flow cytometry to diagnostic pathology. *Lab Invest* 50:115–140, 1984.
36. Ploem-Zaajer JJ, van Driel-Kulker AM, Mesker WE, Cornelisse CJ: Advantages and limitations of retrospective DNA cytometry by flow and image analysis. In Burger G, Ploem JS, Goerttler K (eds): *Clinical Cytometry and Histometry.* London, Academic Press, 1987, pp 176–179.
37. Abmayr W, Deml E, Oesterle D, Gössner W: Nuclear morphology in preneoplastic lesions of rat liver. *Anal Quant Cytol* 5:275–284, 1983.
38. Nickerson JA, Krochmalnic G, Wan KM, Penman S: Chromatin architecture and nuclear RNA. *Cell Biol* 86:177–181, 1989.
39. Haralick RM, Shanmugam K, Dinstein I: Textural features for image classification. *IEEE Trans Syst Man Cybernet* 3:610–621, 1973.
40. Cox KH, De Leon DV, Angerer LM, Angerer RC: Detection of mRNAs in sea urchin embryos by in situ hybridization using asymmetric RNA probes. *Develop Biol* 101:485–502, 1984.
41. Majzoub JA, Rich A, Van Boom J, Habener JF: Vasopressin and oxytocin mRNA regulation in the rat assessed by hybridization with synthetic oligonucleotides. *J Biol Chem* 258:14061–14064, 1983.
42. Stolz W, Scharffetter K, Abmayr W, Köditz W, Krieg T: An automatic analysis method for in situ hybridization using high-resolution image analysis. *Arch Dermatol Res* 281:336–341, 1989.
43. Braverman MS, Braverman IM: Three-dimensional reconstructions of objects from serial sections using a microcomputer graphics system. *J Invest Dermatol* 86:290–294, 1986.
44. Smolle J, Helige C, Soyer HP: Quantitative evaluation of melanoma cell invasion in three dimensional confrontation cultures in vitro using automated image analysis. *J Invest Dermatol* 94:114–119, 1990.
45. Smolle J, Smolle-Juettner FM, Stettner H, Kerl H: Relationship of tumor cell motility and morphologic patterns: 1. Melanocytic skin tumors. *Am J Dermatopathol.* 14:231–237, 1982.
46. Smolle J, Hofmann-Wellenhof R, Kerl H: Prognostic significance of proliferation and motility in primary malignant melanoma of the skin. *J Cutan Pathol* 19:110–115, 1992.
47. Smolle J, Grimstad IA: Tumor-cell motility and invasion within tumors determined by applying computer simulation to histologic patterns. *Int J Cancer* 50:331–335, 1992.
48. Howard V: Rapid nuclear volume estimation in malignant melanoma using point sampled analysis of particles of arbitrary shape. In Mary JY, Rigaut JP (eds): *Quantitative Image Analysis in Cancer Cytology and Histology.* New York, Elsevier Science, 1986, pp 245–256.
49. Lindholm C, Hofer PA: Caryometry of benign compound acquired naevi, Spitz epitheloid naevi, and malignant melanomas. *Acta Pathol Microbiol Immunol Scand (A)* 94:371–374, 1986.
50. Brüngger A, Cruz-Orive LM: Nuclear morphometry of nodular malignant melanomas and benign nevocytic nevi. *Arch Dermatol Res* 279:412–414, 1987.
51. Stolz W, Schmoeckel C, Ryckmanns F, Groß J, Braun-Falco O: Morphometric and ultrastructural analyses of melanocytes, nevus cells, and melanoma cells. *Arch Dermatol Res* 279:167–172, 1987.
52. Stolz W, Groß J, Schmoeckel C, Abmayr W, Braun-Falco O: Which is the best ultrastructural morphometric parameter differentiating between intra-

epidermal melanocytic cells of benign and malignant melanomas? In Burger G, Ploem JS, Goerttler K (eds): *Clinical Cytometry and Histometry.* London, Academic Press, 1987, pp 523–526.
53. Smolle J, Soyer HP, Kerl H: Nuclear parameters of the superficial and deep portion of melanocytic lesions—A morphometric investigation. *Pathol Res Pract* 183:266–270, 1988.
54. Rhodes AR, Seki Y, Fitzpatrick TB, Stern RS: Melanosomal alterations in dysplastic melanocytic nevi. A quantitative, ultrastructural investigation. *Cancer* 61:358–369, 1988.
55. Olinici CD, Giurgiuman M: Morphometric studies on melanocytic tumors. *Morphol Embryol* 35:49–52, 1989.
56. Sorensen FB: Stereological estimation of nuclear volume in benign melanocytic lesions and cutaneous malignant melanomas. *Am J Dermatopathol* 11(6):517–527, 1989.
57. Sorensen FB, Kristensen IB, Grymer F, Jakobsen A: DNA level, tumor thickness, and stereological estimates of nuclear volume in stage I cutaneous malignant melanoma. *Am J Dermatopathol* 13(1): 11–19, 1991.
58. Leitinger G, Cerroni L, Soyer HP, Smolle J, Kerl H: Morphometric diagnosis of melanocytic skin tumors. *Am J Dermatopathol* 12(5):441–445, 1990.
59. Giannini A, Urso C, Santucci M, Bondi R: Benign melanocytic lesions. A morphometric analysis. *Pathol Res Pract* 183:262–265, 1988.
60. Schmiegelow P, Schroiff R, Breitbart E, Bahnsen J, Lindner J, Jänner M: Malignant melanoma—Its precursors and its topography of proliferation. DNA-Feulgen-cytophotometry and mitotic index. *Virchows Arch A (Pathol Anat)* 409:47–59, 1986.
61. Lindholm C, Bjelkenkrantz K, Hofer P: DNA-cytophotometry of benign compound and intradermal naevi, Spitz epitheloid naevi and malignant melanomas. *Virchows Arch B* 53:257–258, 1987.
62. LeBoit PE, Van Fletcher H: A comparative study of Spitz nevus and nodular malignant melanoma using image analysis cytometry. *J Invest Dermatol* 88: 753–757, 1987.
63. Bergman W, Ruiter DJ, Scheffer D, van Vloten WA: Melanocytic atypia in dysplastic nevi. Immunohistochemical and cytophotometric analysis. *Cancer* 61:1660–1666, 1988.
64. Stolz W, Vogt T, Abmayr W, Landthaler M, Hempfer S, Bingler P: Differentiation between malignant melanoma and benign melanocytic nevi by computerized DNA-image cytometry. Unpublished.
65. Fleming MG, Wied GL, Dytch HE: Image analysis cytometry of dysplastic nevi. *J Invest Dermatol* 95:287–291, 1990.
66. Sondergaard K, Larsen JK, Moller U, Christensen IJ, Hou-Jensen K: DNA ploidy characteristics of human malignant melanoma analysed by flow cytometry and compared with histology and clinical course. *Virchows Arch B (Cell Pathol)* 42:53–64, 1983.
67. Büchner T, Hiddemann W, Wörmann B, Kleinemeier B: Differential pattern of DNA-aneuploidy in human malignancies. *Pathol Res Pract* 179:310–317, 1985.
68. Von Roenn JH, Kheir SM, Wolter JM, Coon JS: Significance of DNA abnormalities in primary malignant melanoma and nevi: A retrospective flow cytometric study. *Cancer Res* 46:3192–3195, 1986.
69. Newton JA, Camplejohn RS, McGibbon DH: The flow cytometry of melanocytic skin lesions. *Br J Cancer* 58:606–609, 1988.
70. Kamino H, Ratech H: Improved detection of aneuploidy in malignant melanoma using multiparameter flow-cytometry for S100 protein and DNA content. *J Invest Dermatol* 93:392–396, 1989.
71. Steijlen PM, Hamm H, Van Erp PEJ, Johnson JP, Ruiter DJ, Bröcker EB: Immunohistologic evidence for the malignant potential of congenital melanocytic nevi. *J Invest Dermatol* 92:366–370, 1989.
72. Chi HI, Ishibashi Y, Shima A, Mihara I, Otsuka F: Use of DAPI cytofluorometric analysis of cellular DNA content to differentiate Spitz nevus from malignant melanoma. *J Invest Dermatol* 95:154–157, 1990.
73. Slater SD, Cook MG, Fisher C, Wright NAW, Foster CS: A comparative study of proliferation indices and ploidy in dysplastic naevi and malignant melanomas using flow cytometry. *Histopathol* 19: 337–344, 1991.
74. Sangueza OP, Hyder DM, White CR, et al: Comparison of image analysis with flow cytometry for DNA content analysis in pigmented lesions of the skin. *Anal Quant Cytol Histol* 14:55–59, 1992.
75. Rode J, Williams RA, Jarvis LR, Dhillon AP, Jamal O: S100 protein, neurone specific enolase, and nuclear DNA content in Spitz naevus. *J Pathol* 161:41–45, 1990.
76. Stolz W, Abmayr W, Schmoeckel C, Landthaler M, Massoudy P, Braun-Falco O: Ultrastructural discrimination between malignant melanomas and benign nevocytic nevi using high-resolution image and multivariate analysis. *J Invest Dermatol* 97:903–910, 1991.
77. Stolz W, Abmayr W, Hempfer S, et al: Computer aided quantification of nuclear morphology for the recognition of initial malignant melanoma in light microscopy. Unpublished.

78. Tan GJ, Baak JP: Evaluation of prognostic characteristics of stage I cutaneous malignant melanoma. *Anal Quant Cytol* 3:147–154, 1984.
79. Lindholm C, Hofer PA, Jonsson H: Karyometric findings and prognosis of stage I cutaneous malignant melanomas. *Acta Oncol* 27:227–233, 1988.
80. Gamel JW, McLean IW: Computerized histopathologic assessment of malignant potential: 2. A practical method for predicting survival following enucleation for uveal melanoma. *Cancer* 52:1032–1038, 1983.
81. Srivastava A, Laidler P, Davies RP, Horgan K, Hughes LE: The prognostic significance of tumor vascularity in intermediate thickness (0.76–4.0 mm thick) skin melanoma. *Am J Pathol* 133:419–423, 1988.
82. Gamel JW, Greenberg RA, McLean IW, et al: A clinically useful method for combining gross and microscopic measurements to select high-risk patients after enucleation for ciliochoroideal melanoma. *Cancer* 57:1341–1344, 1986.
83. Tosi P, Frezzotti R, Cintorino M, et al: Quantitative morphological parameters for evaluating the propensity of choroidal melanomas to orbital extension. *Orbit* 6:139–145, 1987.
84. Gebhart W, Knobler R: Computer-assisted volumetric analysis of cutaneous malignant melanomas. *Am J Dermatopathol* 6:93–95, 1984.
85. Donoso JW, Augsburger JJ, Shields JA, Greenberg RA, Gamel JW: Metastatic uveal melanoma. Correlation between survival time and cytomorphometry of primary tumors. *Arch Ophthalmol* 104:76–78, 1986.
86. Hansson J, Tribukait B, Lewensohn R, Ringborg U: Flow cytofluorometric DNA analyses of metastases of human malignant melanomas. *Anal Quant Cytol* 4:99–104, 1982.
87. Frankfurt OS, Greco WR, Slocum HK, et al: Proliferative characteristics of primary and metastatic human solid tumors by DNA flow cytometry. *Cytometry* 5:629–635, 1984.
88. Kheir SM, Bines SD, von Roenn JH, Soong SJ, Urist MM, Coon JS: Prognostic significance of DNA aneuploidy in stage I cutaneous melanoma. *Ann Surg* 207:455–461, 1988.
89. Bines SD, von Roenn JH, Kheir SM, Coon JS: Flow cytometry in melanoma. In Nathanson L (ed): *Malignant Melanoma: Biology, Diagnosis, and Therapy.* Boston, Kluwer Academic Publishers, 1988. pp 155–169.
90. Bartkowiak D, Otto F, Schuman J, Lippold A, Drepper H: Sequential DNA flow cytometry in metastatic malignant melanoma. *Oncology* 48:154–157, 1991.
91. Zaloudik J, Moore M, Ghosh AK, Mechl Z, Rejthar A: DNA content and MHC class II antigen expression in malignant melanoma: Clinical course. *J Clin Pathol* 41:1078–1084, 1988.
92. Rode J, Williams RA, Dhillon AP, Moss E: Nuclear DNA profiles in primary melanomas and their metastases. *Cancer* 67:2333–2336, 1991.
93. Gattuso P, Reddy V, Solans E, et al: Is DNA ploidy of prognostic significance in stage I cutaneous melanoma? *Surgery* 108:702–709, 1990.
94. Heenan PJ, Jarvis LR, Armstrong BK: Nuclear indices and survival in cutaneous melanoma. *Am J Dermatopathol* 11:308–312, 1989.
95. Vogt T, Stolz W, Abmayr W, Bingler P, Landthaler M: Prognostic significance of DNA cytometry in malignant melanoma. Unpublished.
96. Lindholm C, Hofer PA, Jonsson H: Single cell DNA cytophotometry in clinical stage I malignant melanoma. Relationship to prognosis. *Acta Oncol* 29:147–150, 1990.
97. Zeng QS, Fu YS, Alistair A, Cochran J: Nuclear DNA measurements of metastatic melanoma by a computerized digital imaging system. *Hum Pathol* 21:1112–1116, 1990.
98. Schmiegelow P, Oppermann T, Nüßgen A, Schroiff R, Jänner M: Melanoma in situ adjacent to an invasive nodular melanoma and metastases—DNA-cytophotometry, mitotic index, and anisokaryosis. *Virchows Arch A (Pathol Anat)* 411:871–873, 1987.
99. Onishi K, Ishikawa H: Flow cytometric DNA analysis of primary cutaneous malignant melanoma. *Acta Derm Venerol Stockh* 71:525–528, 1991.
100. Björnhagen V, Auer G, Lagerlöf B, Erhardt K, Mansson-Brahme E: Nuclear DNA analyses in archival material from primary malignant melanoma. A pilot study. *Anal Quant Cytol Histol* 13: 335–342, 1991.
101. MacDonald DM: Histopathological differentiation of benign and malignant cutaneous lymphocytic infiltrates. *Br J Dermatol* 107:715–718, 1982.
102. Brodell RT, Santa Cruz DJ: Cutaneous pseudolymphomas: Symposium on cutaneous T-cell lymphomas and related disorders. *Dermatol Clin* 4:719–734, 1985.
103. Payne CM, Grogan TM, Lynch PJ: An ultrastructural morphometric and immunohistochemical analysis of cutaneous lymphomas and benign lymphocytic infiltrates of the skin: Useful criteria for diagnosis. *Arch Dermatol* 122:1139–1154, 1986.
104. Wantzin GL, Larsen JK, Christensen J, Ralfkiaer E, Thomsen K: Early diagnosis of cutaneous T-cell lymphoma by DNA flow cytometry on skin biopsies. *Cancer* 54:1348–1352, 1984.

105. Van Vloten WA, van Duijn P, Schaberg A: Cytodiagnostic use of Feulgen-DNA measurements in cell imprints from the skin of patients with mycosis fugoides. *Br J Dermatol* 91:365–371, 1974.
106. Van Vloten WA, Willemze R: New techniques in the evaluation of cutaneous T-cell lymphomas: Symposium on cutaneous T-cell lymphomas and related disorders. *Dermatol Clin* 4:665–672, 1985.
107. Stolz W, Vogt T, Braun Falco O, Abmayr W, Eckert F, Kaudewitz P, Vieluf D, Bieber K, Burg G: Differentiation between lymphomas and pseudolymphomas of the skin by computerized DNA-image cytometry. *J Invest Dermatol* 94:254–260, 1990.
108. Böcking A, Adler C-P, Common HH, Hilgart M, Granzen B, Auffermann W: Algorithm for a DNA-cytophotometric diagnosis and grading of malignancy. *Anal Quant Cytol* 6:1–8, 1984.
109. Meijer CJLM, van der Loo EM, Scheffer E, Cornelisse CJ, van Vloten WA: Relevance of morphometry in the diagnosis and prognosis of cutaneous T-cell lymphomas. In Goos M, Christophers E (eds): *Lymphoproliferative Diseases of the Skin.* Berlin, Springer-Verlag, 1982, pp 117–127.
110. Willemze R, Cornelisse CJ, Hermanns J, Pardoel VPAM, van Vloten WA, Meijer CJLM: Quantitative electron microscopy in early diagnosis of cutaneous T-cell lymphomas. *Am J Pathol* 123:166–173, 1986.
111. Lessin SR, Grove GL, Diamond LW, Au FC, Nowell PC, Vonderheid EC: DNA cytophotometry of lymph node touch imprints in cutaneous T-cell lymphoma. *J Invest Dermatol* 90:425–429, 1988.
112. Thomsen K, Lange Wantzin G: Lymphomatoid papulosis. A follow up study of 30 patients. *J Am Acad Dermatol* 17:632–636, 1987.
113. Willemze R, Meijer CJLM, van Vloten WA, Scheffer E: The clinical and histological spectrum of lymphomatoid papulosis. *Br J Dermatol* 107:131–144, 1982.
114. Lange Wantzin G, Larsen JK, Christensen IJ, Ralfkiaer E, Thomsen K: Early diagnosis of cutaneous T-cell lymphomas by DNA flow cytometry on skin biopsies. *Cancer* 54:1348–1352, 1984.
115. Ralfkiaer E, Lange Wantzin G, Larsen JK, Christensen IJ, Thomsen K: Single cell DNA-measurements in benign cutaneous lymphoid infiltrates and in positive patch test. *Br J Dermatol* 112:253–262, 1985.
116. Joensuu H, Klemi PJ, Eerola E: Diagnostic value of DNA flow cytometry combined with fine needle aspiration in lymphomas. *J Pathol* 154:237–245, 1988.
117. Pastel-Levy C, Flotte TJ, Preffer F, et al: Application of DNA flow cytometry from paraffin-embedded tissue to the diagnosis of mycosis fungoides. *Cutan Pathol* 18:279–283, 1991.
118. Vonderheid EC, Fang S-M, Helfrich MK, Abraham SR, Nicolini CA: Biophysical characterization of normal T-lymphocytes and Sézary cells. *J Invest Dermatol* 76:28–37, 1981.
119. Burger G, Jütting U, Gais P, et al: The role of chromatin pattern in automated cancer cytopathology. In Mary JY, Rigaut JP (eds): *Quantitative Image Analysis in Cancer Cytology and Histology.* Amsterdam, Elsevier, 1986, pp 91–102.
120. Robinson D, Lackie P, Aber V, Catovsky D: Morphometric analysis of chronic B-cell leukemias—An aid to the classification of lymphoid cell types. *Leukemia Res* 13:357–365, 1989.
121. Pelstring RJ, Swerdlow SH: Morphometric analysis of follicular center cells: A new approach. *Mod Pathol* 1:262–267, 1988.
122. Lennert K, Mohri N: *Malignant Lymphomas.* Berlin, Springer, 1978.
123. Krüger GR, Medina JR, Klin HO, et al: A new working formulation of non-Hodgkin lymphomas. A retrospective study of the new NC classification proposal in comparison to the Rappaport and Will classification. *Cancer* 52:833–840, 1983.
124. Burg G, Braun-Falco O: *Cutaneous Lymphomas, Pseudolymphomas, and Related Disorders.* New York, Springer, 1983, pp 81–93.
125. Kerl H, Hödl S, Smolle J, Konrad K: Klassifikation und Prognose kutaner T-Zell-Lymphome. *Z Hautkr* 61:63–67, 1986.
126. Vogt T, Stolz W, Braun-Falco O, et al: Prognostic significance of DNA cytometry in cutaneous malignant lymphomas. *Cancer* 68:1095–1100, 1991.
127. Smolle J, Stolz W, Bahmer FA, et al: Analytical morphology in dermatology—Technical aspects and practical applications. Unpublished.
128. Herzberg AJ, Kerns BJ, Pollack SV, Kinney RB: DNA image cytometry of keratoacanthoma and squamous cell carcinoma. *J Invest Dermatol* 97:495–500, 1991.
129. Sanchez MA, Ames ED, Erhardt K, Auer GU: Analysis of DNA distribution in Kaposi's sarcoma in patients with and without the aquired immune deficiency syndrome. *Anal Quant Cytol Histol* 10:16–20, 1988.
130. Stolz W, Schmid R, Ring J, Landthaler M, Braun Falco O: Ist das epidemische Kaposi-Sarkom primär neoplastisch? DNA-zytometrische Untersuchungen (abstract) 2. Deutscher AIDS Kongress, Berlin, 1989.
131. Braverman IM, Keh-Yen A: Three-dimensional reconstruction of endothelial cell gaps in psoriatic

vessels and their morphologic identity with gaps produced by the intradermal injection of histamine. *J Invest Dermatol* 86:577–581, 1986.

132. Braverman IM, Sibley J, Keh A: Ultrastructural analysis of the endothelial-pericyte relationship in diabetic cutaneous vessels. *J Invest Dermatol* 95: 147–153, 1990.
133. Lindelöf B, Forslind B, Hedblad M-A, Kaveus U: Human hair form. Morphology revealed by light and scanning electron microscopy and computer aided three-dimensional reconstruction. *Arch Dermatol* 124:1359–1363, 1988.
134. Ito M, Hashimoto K, Katsuumi K, Sato Y: Pathogenesis of monilethrix: Computer stereography and electron microscopy. *J Invest Dermatol* 95:186–194, 1990.
135. Scheynius A, Lundahl P: Three-dimensional visualization of human Langerhans cells using confocal scanning laser microscopy. *Arch Dermatol Res* 281: 521–525, 1990.
136. Lang PG, McKelvey AC, Nicholson JH: Three-dimensional reconstruction of the superficial multicentric basal cell carcinoma using serial sections and a computer. *Am J Dermatopathol* 19:198–203, 1987.
137. Lea PJ, Pawlowski A: Human melanocytic nevi: 1. Electronmicroscopy and 3-dimensional computer reconstruction of naevi and basement membrane zone from ultrathin serial sections. *Acta Derm Venerol (Stockh)* 127(suppl):5–15, 1986.
138. Dhawan AP: An expert system for the early detection of melanoma using knowledge-based image analysis. *Anal Quant Cytol Histol* 10:405–416, 1988.

TWELVE COMPUTER APPLICATIONS IN DERMATOLOGY EDUCATION

Charles A. Sneiderman and William V. Stoecker

In a forest a fox bumps into a little rabbit, and says, "Hi, junior, what are you up to?"
"I'm writing a dissertation on how rabbits eat foxes," said the rabbit.
"Come now, friend rabbit, you know that's impossible!"
"Well, follow me and I'll show you." They both go into the rabbit's dwelling and after a while the rabbit emerges with a satisfied expression on his face. Comes along a wolf. "Hello, what are we doing these days?"
"I'm writing the second chapter of my thesis, on how rabbits devour wolves."
"Are you crazy? Where is your academic honesty?"
"Come with me and I'll show you." As before, the rabbit comes out with a satisfied look on his face and a diploma in his paw. Finally, the camera pans into the rabbit's cave and, as everybody should have guessed by now, we see a mean-looking, huge lion sitting next to some slight remnants of the wolf and the fox.
Moral: It's not the contents of your thesis that are important—it's your PhD advisor that really counts.

—Unattributed login message, SUN OS 4.1.1 UNIX, U MO-Rolla, September 11, 1992

EVOLUTION OF COMPUTERS IN MEDICAL EDUCATION

Although electronic computers were used as early as the 1960s to model physiologic processes and differential diagnosis, the application of computers to medical education was catalyzed by the development of hardware and software capable of storing and retrieving text as well as arithmetic data during the 1970s.[1] The dedicated minicomputer made real-time interaction possible between a learner sitting at a CRT (cathode ray tube) terminal and such pioneering sites as the Massachusetts General Hospital Laboratory of Computer Science and the Ohio State University via communications networks. These systems allowed the learner to get immediate feedback on drill-and-practice and problem-solving questions without requiring any computer skills beyond the ability to type at a keyboard.[2] However it was not until the proliferation of the microcomputer during the past decade that the profession has begun to consider the computer as a utility rather than a novelty in medical education.

Evolution of Hardware

The evolution of hardware over the past three decades has allowed a migration of the learning center from a remote area of the medical center to the coat pocket of the learner. Prior to the 1960s, interaction between learners and computer programs was impossible; all computers required that both data and programs to manipulate the data be entered on punched cards or magnetic tape. In the 1960s, the development of teletype (TTY) terminals enabled interactive data entry into existing prograns so that nonprogrammers could use typewriter keyboards and get responses within minutes. The TTYs could be cabled over short distances from a room-sized "mainframe," which had to be housed in a remote area of the medical center where it could be cooled by a massive air conditioner and powered by high voltage current. By the 1970s, CRT terminals that could transmit and receive data in seconds became commonplace. CRTs could be networked across the medical campus to a departmentalized refrigerator-sized "minicomputer," which could time-share computer-assisted instruction with other tasks. Since the 1980s, "microcomputers" have evolved in a magic "breadbox" that daily becomes smaller, cheaper, faster, and more versatile.

The development of optical disk storage (a technique in which a modulated laser beam encodes and retrieves data from a thin metal film on an inexpensive plastic platter as in Chapter 3) has dra-

matically reduced the cost of reproducing and distributing large databases. Now alphanumeric data, images, and sound can be all be recorded on these plastic disks. Information that formerly was only practical to broadcast from a central source to remote sites can now be inexpensively distributed and accessed locally. Depending on the format of both the disk and laser reader, audio, video, and digital data may require separate peripheral devices, but all can be controlled by a microcomputer for multimedia presentation.

Evolution of Software

Similarly, instructional software has evolved as operating systems and higher-level programming languages have made applications programming (Fig. 4-1) easier. In the 1960s, data-independent programming languages with branching logic that could support interactive question-and-answer sessions became readily available. In the 1970s, database management software supporting alphabetic string searching, variable-length field text retrieval, and relational structures was applied to models of diagnostic reasoning. In the 1980s, authoring packages with menu or graphical icon interfaces were developed that supported "computer illiterate" content experts in creating multimedia simulations of clinical interactions. Today software handling fuzzy logic, object-oriented data structure, and graphical user interfaces may allow learners to navigate such difficult tasks as visualizing spatial anatomic relationships through "artificial reality."

Evolution of Educational Methods

Without supporting hardware and software, courseware development was limited to the technology of the day. Thus in the 1960s, simulation of quantitative processes and multiple-choice drill and practice were the repertoire of computer-assisted instruction (CAI) in medicine. In the 1970s, text-based simulation of diagnostic and therapeutic reasoning was novel. In the 1980s, the development of tools for hypertext (the ability to move within a database without negotiating through a hierarchical structure) together with developments in peripheral hardware to produce sounds and images made multimedia databases a popular paradigm.

Evaluation of Computer-Assisted Instruction

A century ago, Abraham Flexner proposed the American model for medical education set in classroom, laboratory, and hospital bedside teaching.[3] Today the classroom must accommodate an increasing factual knowledge base of human form and function from molecule to society; the laboratory must allow students to practice their skills on an increasingly scarce supply of human and animal tissue; and the bedside can show only that glimpse of the clinical spectrum that benefits from the high technology of the contemporary hospital. These settings are now themselves domains of the information age, with computer hardware being used for administration, communication, patient care, and research.

CAI in these settings has become an adjunct to such traditions as lecture, demonstration, and practice. CAI can document acquisition of knowledge and skills and accommodate to individual schedules and pace of learning. There is ample evidence that CAI results in more time-efficient learning, although there is no evidence that knowledge or skills acquired exceed those acquired by conventional methods.[4] Although CAI is well-received by students, CAI production requires a major commitment of instructional design, content analysis, and programming effort. Faculty resistance to CAI may occur if there is an implication that current instruction is ineffective or if the technology is unfamiliar; faculty participation in development is necessary but not sufficient to a successful CAI project.[5]

It is most telling that incoming medical students are now required to bring microcomputers rather than microscopes as the required learning tool.

APPLICATIONS IN MEDICAL EDUCATION

Although it is impossible in print media to recreate the experience of computer-based education, we will attempt to review several current themes and exemplary projects that offer education relevant to cutaneous medicine and represent developments in the field.

Tutorials

AI/LEARN/RHEUMATOLOGY is a tutorial on the rheumatic diseases that offers students stepwise